Energy Efficiency of the Cell-Free Massive MIMO Uplink with Optimal Uniform Quantization

Energy Efficiency of the Cell-Free Massive MIMO Uplink with Optimal Uniform Quantization

Manijeh Bashar, *Student Member, IEEE*, Kanapathippillai Cumanan, *Member, IEEE*, Alister G. Burr, *Senior Member, IEEE*, Hien Quoc Ngo, *Member, IEEE*, Erik G. Larsson, *Fellow, IEEE*, and Pei Xiao, *Senior Member, IEEE*

Abstract

A cell-free Massive multiple-input multiple-output (MIMO) uplink is considered, where the access points (APs) are connected to a central processing unit (CPU) through limited-capacity wireless microwave links. The quantized version of the weighted signals are available at the CPU, by exploiting the Bussgang decomposition to model the effect of quantization. A closed-form expression for spectral efficiency is derived taking into account the effects of channel estimation error and quantization distortion. The energy efficiency maximization problem is considered with per-user power, backhaul capacity and throughput requirement constraints. To solve this non-convex problem, we decouple the original problem into two sub-problems, namely, receiver filter coefficient design and power allocation. The receiver filter coefficient design is formulated as a generalized eigenvalue problem whereas a successive convex approximation (SCA) and a heuristic sub-optimal scheme are exploited to convert the power allocation problem into a standard geometric programming (GP) problem. An iterative algorithm is proposed to alternately solve each sub-problem. Complexity analysis and convergence of the proposed schemes are investigated. Numerical results indicate the superiority of the proposed algorithms over the case of equal power allocation.

***Keywords*:** Cell-free Massive MIMO, Bussgang decomposition, convex optimization, energy efficiency, geometric programming, generalized eigenvalue problem.

I. Introduction

In recent years, several novel technologies have been identified for the design of fifth generation (5G) radio access networks (RANs) to deliver a wide range of new user services and to meet the dramatical increase of network spectral and energy efficiencies. Massive multiple-input multiple-output (MIMO) and cloud RAN (C-RAN) have been recognized as two of the key elements of 5G systems. In C-RAN, the remote radio heads (RRHs) are distributed across the coverage area and the base-band processing is carried out at central base band unit (BBU). In cellular networks,

M. Bashar, K. Cumanan and A. G. Burr and are with the Department of Electronic Engineering, University of York, Heslington, YO10 5DD, York, UK. e-mail: {mb1465, kanapathippillai.cumanan, alister.burr}@york.ac.uk. M. Bashar is also with home of the 5G Innovation Centre, Institute for Communication Systems, University of Surrey, UK. e-mail: m.bashar@surrey.ac.uk.

H. Q. Ngo is with the School of Electronics, Electrical Engineering and Computer Science, Queen's University Belfast, BT3 9DT, Belfast, UK. e-mail: hien.ngo@qub.ac.uk.

E. G. Larsson is with the Department of Electrical Engineering, Linköping University, 581 83 Linköping, Sweden. e-mail:erik.g.larsson@liu.se.

Pei Xiao is with home of the 5G Innovation Centre, Institute for Communication Systems, University of Surrey, UK. e-mail: p.xiao@surrey.ac.uk.

The work of A. G. Burr and K. Cumanan was supported by H2020-MSC ARISE-2015 under Grant 690750.

Parts of this work was presented at the IEEE ICC 2019 [1].

the area is divided into several cells with one base station (BS) in each cell and each BS only serves users distributed in its cell. The bottleneck in cellular networks is the performance of cell edge users [2]. To deal with this problem, cell-free Massive MIMO is introduced. In cell-free Massive MIMO, there are no cells, and hence, no boundaries. All users in the network are coherently served by many access points (APs) via a central processing unit (CPU) [3]–[5]. In [6] a user-centric approach is proposed where each user is served by a small number of APs. Cell-free Massive MIMO effectively implements a user-centric approach [7]. Moreover, the effect of hardware impairments on cell-free Massive MIMO is investigated in [8].

Cell-free Massive MIMO is a scalable and practical version of network MIMO or coordinated multipoint processing (CoMP) [9], which combines Massive MIMO technology and C-RAN. The authors in [10], [11] present an overview of the basics of CoMP. The authors in [12] investigate the performance of CoMP with statistical channels. Moreover, the performance of CoMP with limited capacity backhaul links is investigated in [13], [14]. Massive MIMO technology exploits the favorable propagation and channel hardening properties to offer huge spectral and energy efficiencies with simple linear processing whereas C-RAN provides an opportunity for the network operators to implement RANs without encountering inter-cell interference. Note that the analysis of favorable propagation and channel hardening in cell-free Massive MIMO is presented in [15]. The backhaul load is one of the key issues that needs to be addressed in any distributed antenna systems [16]–[18]. As such, the implementation of cell-free Massive MIMO with limited backhaul links is the main challenge in the uplink mode, as the limited backhaul links forward the received signal from the APs to the CPU. When converted to digital form this requires a capacity for the backhaul links many times the corresponding user data rate, to ensure signals are transferred with sufficient precision. In the C-RAN literature this has been estimated as 20-50 times the corresponding data rate, implemented using the common public radio interface (CPRI) standard [19], typically over optical fiber [20].[1] The assumption of infinite backhaul in [3] is not realistic in practice. It is reasonable to assume, however, that the fronthaul network will carry quantized signals, at least in the uplink direction, and that this will affect the network performance. Therefore, this paper provides an approach for the analysis of the effect of backhaul quantization on the uplink of cell-free Massive MIMO. While there has been

[1]Note that in [20, page 12], the authors present various calculations for the backhaul load. The factor 20-50 times does not appear, but (for example) it suggests that GSM would require 25.6 Mbps - since GSM can send at most 280 kbit/s this would be more like 100 times.

significant work in the context of network MIMO on compression techniques such as Wyner-Ziv coding for interconnection of BSs, here for simplicity (and hence improved scalability) we assume simple uniform quantization. The non-uniform additive quantization noise model (AQNM) quantizer is investigated in [21], [22]. In this paper, we assume that the correlation between the input signals of the quantizers at the different APs is negligible. Note that the authors in [23] investigate the effect of correlation across the antennas in collocated Massive MIMO. We exploit the Bussgang decomposition [24] to model the effect of quantization. We study the case when only the quantized version of the weighted signal is available at the CPU and the CPU employs maximum-ratio combining (MRC) detection. Similar to the model in [25], the backhaul links establish communications through wireless microwave links with limited capacity. Next, we derive the backhaul rate of cell-free Massive MIMO. For a given backhaul capacity, we show that the relative total power consumption in the cell-free Massive MIMO system depends on the length of uplink pilot vectors, channel coherence time and the total number of quantization bits. The uplink energy efficiency of the cell-free Massive MIMO system is investigated in this paper. In particular, optimal power allocation strategies which maximize the uplink energy efficiency are investigated for a system in which the quantized version of the weighted signals obtained from MRC weighting at APs are available at the CPU. The contributions of the paper are summarized as follows:

1. An expression for uplink energy efficiency is derived based on channel statistics and taking into account the effects of channel estimation errors, the effect of pilot sequences, and quantization distortion.
2. We exploit the Bussgang decomposition to model the effect of quantization and present the analytical solution to find the optimal step-size of the quantizer.
3. A novel approach to solve the non-convex energy efficiency maximization problem is proposed, where we propose to decompose the original problem into two sub-problems and an iterative algorithm is developed to determine the optimal solution. An successive convex approximation (SCA) is used to efficiently solve the power allocation problem. Next, a heuristic sub-optimal energy efficiency maximization problem is proposed where the original optimization problem is transformed into a standard geometric programming (GP).
4. The convergence and complexity analysis of the proposed schemes are presented. The

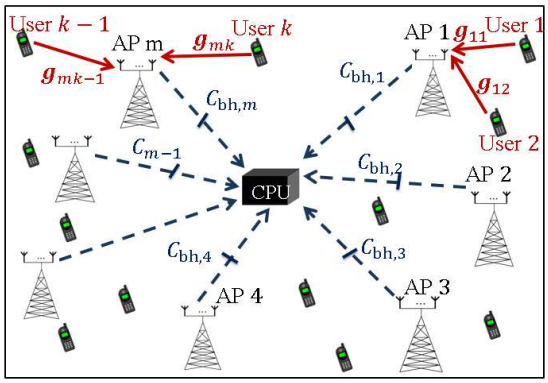

Figure 1. The uplink of a cell-free Massive MIMO system with *K* single-antenna users and *M* APs. Each AP is equipped with N antennas. The solid lines denote the uplink channels and the dashed lines present the limited capacity backhaul links between the APs and the CPU.

numerical results confirm that the proposed algorithm converges after a few iterations.

5. Numerical results demonstrate that the proposed scheme substantially outperforms the case with equal power allocation. Moreover, numerical results demonstrate that although the proposed sub-optimal scheme has a lower complexity, it provides a performance fairly close to the SCA scheme.

A. *Outline*

The rest of the paper is organized as follows. Section II describes the system model and Section III provides performance analysis. The total energy efficiency model is presented in Section IV and the proposed total energy efficiency maximization scheme is provided in Section V. Numerical results are provided in Section VI, and finally Section VII concludes the paper.

B. *Notation*

It is assumed that $x \sim \mathcal{CN}(0, \sigma^2)$ represents a zero-mean circularly symmetric complex Gaussian random variable with variance σ^2. The conjugate of the variable x is presented by x^*. Moreover, $[\mathbf{x}]_n$, $\mathcal{R}(x)$ and $\mathcal{I}(x)$ represent the nth element of vector $\mathbf{x}$, the real part and imaginary part of the complex variable x, respectively. Finally, diag$[\mathbf{x}]$ refers to a diagonal matrix whose diagonal elements are the elements of vector $\mathbf{x}$.

II. SYSTEM MODEL

We consider uplink transmission in a cell-free Massive MIMO system with M APs and K single-antenna users randomly distributed in a large area, as shown in Fig. 1. Moreover, we assume each AP has N antennas. The channel coefficient vector between the kth user and

the mth AP, $\mathbf{g}_{mk} \in \mathbb{C}^{N\times 1}$, is modeled as $\mathbf{g}_{mk} = \sqrt{\beta_{mk}}\mathbf{h}_{mk}$, where β_{mk} denotes the large-scale fading and $\mathbf{h}_{mk} \sim \mathcal{CN}(0, \mathbf{I_N})$ represents the small-scale fading [3]. In this paper, we evaluate the performance of cell-free Massive MIMO for a scenario with rich scattering. A possible, alternative model is the Ricean channel. Cell-free Massive MIMO with Ricean fading and quantization errors has not been investigated before, but is out of the scope of this paper. Two closely related works are: [26] that investigates cell-free Massive MIMO with Ricean fading but without quantization errors, and [27] that studies *cellular* Massive MIMO with Ricean channels and with quantization errors.

A. Uplink Channel Estimation

All pilot sequences transmitted by the K users in the channel estimation phase are collected in a matrix $\mathbf{\Phi} \in \mathbb{C}^{\tau_p\times K}$, where τ_p is the length of the pilot sequence for each user and the kth column of $\mathbf{\Phi}$, $\boldsymbol{\phi}_k$, represents the pilot sequence used for the kth user. After performing a de-spreading operation (i.e., projecting the received pilot signal onto $\boldsymbol{\phi}_k$), the minimum mean-square error (MMSE) estimate of the channel coefficient between the kth user and the mth AP is given by [3]

$$\hat{\mathbf{g}}_{mk} = c_{mk}\left(\sqrt{\tau_p p_p}\mathbf{g}_{mk} + \sqrt{\tau_p p_p}\sum_{k'\neq k}^{K}\mathbf{g}_{mk'}\boldsymbol{\phi}_{k'}^H\boldsymbol{\phi}_k + \mathbf{W}_{p,m}\boldsymbol{\phi}_k\right), \tag{1}$$

where $\mathbf{W}_{p,m}$ denotes the noise vector at the mth antenna whose elements are independent and identically distributed (i.i.d) $\mathcal{CN}(0,1)$, p_p represents the normalized signal-to-noise ratio (SNR) of each pilot symbol (which we define in Section VI), and c_{mk} is given by $c_{mk} = \frac{\sqrt{\tau_p p_p}\beta_{mk}}{\tau_p p_p \sum_{k'=1}^{K}\beta_{mk'}|\boldsymbol{\phi}_{k'}^H\boldsymbol{\phi}_k|^2+1}$. Note that, as in [3], we assume that the large-scale fading, β_{mk}, is known.[2] The estimated channels in (1) are used by the APs to design the receiver coefficients.

B. Uplink Transmission

In this subsection, we consider the uplink data transmission, where all users send their signals to the APs. The transmitted signal from the kth user is represented by $x_k = \sqrt{q_k}s_k$, where s_k ($\mathbb{E}\{|s_k|^2\} = 1$) and q_k denotes the transmitted symbol and the transmit power from the kth user, respectively. The $N \times 1$ received signal at the mth AP from all users is given by

$$\mathbf{y}_m = \sqrt{\rho}\sum_{k=1}^{K}\mathbf{g}_{mk}\sqrt{q_k}s_k + \mathbf{n}_m, \tag{2}$$

[2]The large-scale fading β_{mk} changes very slowly with time. Compared to the small-scale fading, the large-scale fading changes much more slowly, some 40 times slower according to [28], [29]. Therefore, β_{mk} can be estimated in advance. One simple way is that the AP takes the average of the power level of the received signal over a long time period. A similar technique for collocated Massive MIMO is discussed in [29, Section III-D].

where $\mathbf{n}_m \in \mathbb{C}^{N\times 1}$ is the noise at the mth AP and ρ is the normalized uplink SNR. We assume that elements of n_m are independent and identically distributed (i.i.d.) $\mathcal{CN}(0,1)$ random variables (RVs).

C. Optimal Uniform Quantization Model

We assume that the in-phase and quadrature components of the weighted signals at each AP are uniformly quantized. The Bussgang theorem [24] is exploited, where a nonlinear output of a quantizer can be introduced by a linear function plus uncorrelated distortion as $\mathcal{Q}(z) = az + n_d,\ \forall k$, where a is a constant, n_d refers to the distortion noise, z is the input of the quantizer [17], [24], [30]–[32]. The term a is given by $a = \frac{\mathbb{E}\{zh(z)\}}{\mathbb{E}\{z^2\}} = \frac{1}{p_z}\int_{\mathcal{Z}} zh(z)f_z(z)d\ z$, where $p_z = \mathbb{E}\{|z|^2\} = \mathbb{E}\{z^2\}$ denotes the power of z and we drop absolute value as z is a real number, and $f_z(z)$ represents the probability distribution function of z. We define the second parameter $b = \frac{\mathbb{E}\{h^2(z)\}}{\mathbb{E}\{z^2\}} = \frac{1}{p_z}\int_{\mathcal{Z}} h^2(z)f_z(z)dz$ [17], [24], [30]. We aim to maximize the signal-to-distortion noise ratio (SDNR), which is defined as follows: $\text{SDNR} = \frac{\mathbb{E}\{(az)^2\}}{\mathbb{E}\{n_d^2\}} = \frac{a^2}{b-a^2}$, where $\mathbb{E}\{az^2\} = a^2 p_z$, and $\mathbb{E}\{n_d^2\} = p_{n_d} = (b-a^2)p_z$. Note that for the midrise uniform quantizer function, the terms a and b are obtained in [30]. In general, terms a and b are functions of the power of the quantizer input, p_z. To remove this dependency, we normalize the input signal by dividing the input signal, z, by the square root of its power, $\sqrt{p_z}$, and then multiply the quantizer output by $\sqrt{p_z}$. Hence, by introducing a new variable $\tilde{z} = \frac{z}{\sqrt{p_z}}$, we have

$$\mathcal{Q}(z) = \sqrt{p_z}\mathcal{Q}(\tilde{z}) = \tilde{a}\sqrt{p_z}\tilde{z} + \sqrt{p_z}\tilde{n}_d = \tilde{a}z + \sqrt{p_z}\tilde{n}_d. \tag{3}$$

The optimal step-size of the quantizer, Δ_{opt}, can be obtained by solving the following maximization problem:

$$\Delta_{\text{opt}} = \arg\max_{\Delta} \text{SDNR} = \arg\max_{\Delta} \frac{a^2}{b-a^2} = \arg\max_{\Delta} \frac{\tilde{a}^2}{\tilde{b}-\tilde{a}^2}. \tag{4}$$

The maximization problem in (4) can be solved through a one-dimensional search over Δ for a given number of quantization bits in a symbolic mathematics tool such as Mathematica [17], [30], and the resulting distortion power are summarized in Table I.

D. Quantization of the Weighted Signal at the APs

The received signal for the kth user is multiplied by the low complexity MRC detector at each AP. Using Bussgang's theorem [24], a nonlinear output can be represented as a linear function as follows:

$$\mathcal{Q}\left(\mathcal{R}\left(\hat{\mathbf{g}}_{mk}^H \mathbf{y}_m\right)\right) = \tilde{a}\mathcal{R}\left(\hat{\mathbf{g}}_{mk}^H \mathbf{y}_m\right) + \sigma_{\mathcal{R}\left(\hat{\mathbf{g}}_{mk}^H \mathbf{y}_m\right)}\tilde{n}_{d,mk},\ \forall k, \tag{5}$$

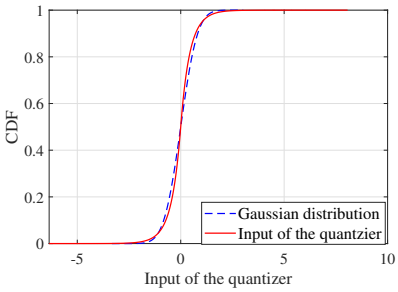

(a) Here $K = 40$, $N = 1$ and $\tau_p = K$.

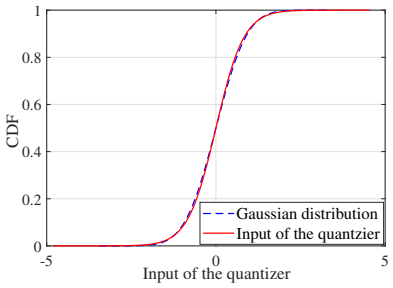

(b) Here $K = 40$, $N = 10$ and $\tau_p = K$.

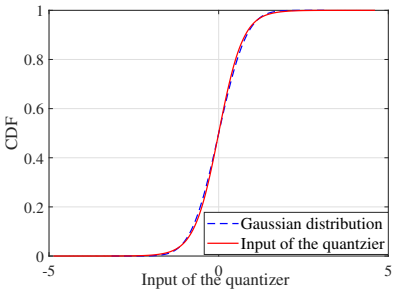

(c) Here $K = 40$, $N = 1$ and $\tau_p = 30$.

Figure 2. Cumulative distribution of the input of the quantizer.

where $\sigma_{\mathcal{R}\left(\hat{\mathbf{g}}_{mk}^H \mathbf{y}_m\right)}$ is the standard deviation of the $\mathcal{R}\left(\hat{\mathbf{g}}_{mk}^H \mathbf{y}_m\right)$. The same equality holds for the imaginary part $\mathcal{I}\left(\hat{\mathbf{g}}_{mk}^H \mathbf{y}_m\right)$. Note that the following equality holds:

$$\sigma^2_{\mathcal{R}\left(\hat{\mathbf{g}}_{mk}^H \mathbf{y}_m\right)} = \sigma^2_{\mathcal{I}\left(\hat{\mathbf{g}}_{mk}^H \mathbf{y}_m\right)} = \frac{1}{2}\sigma^2_{\hat{\mathbf{g}}_{mk}^H \mathbf{y}_m}. \tag{6}$$

Remark 1. *Note that in [33], Bussgang assumes that the input signal of the quantizer has a Gaussian distribution. Since the input of quantizer is the sum of many random variates, from the central limit theorem, it has near Gaussian distribution. Therefore, we use the Bussgang decomposition, making the approximation that the input of the quantizer is Gaussian distributed. The Gaussian approximation can be verified numerically, for typical parameter values, as shown in Fig. 2a-2c. We can see that the cumulative distribution of the empirical distribution matches very well with that of the Gaussian distribution.*

In order to improve the performance, the forwarded signal is further multiplied by the receiver filter coefficients at the CPU. Finally, using the Bussgang decomposition and the receiver filter coefficients $u_{mk}, \forall m, k$ at the CPU, the aggregate received signal at the CPU can be written as

$$r_k = \sum_{m=1}^{M} u_{mk} \mathcal{Q}\left(\hat{\mathbf{g}}_{mk}^H \mathbf{y}_m\right) = \sum_{m=1}^{M} u_{mk} \Bigg(\tilde{a}\ \hat{\mathbf{g}}_{mk}^H \mathbf{y}_m + \underbrace{\sigma_{\hat{\mathbf{g}}_{mk}^H \mathbf{y}_m} \tilde{n}_{d,mk}}_{n_{d,mk}} \Bigg) = \sum_{m=1}^{M} u_{mk} \left(a\ \hat{\mathbf{g}}_{mk}^H \mathbf{y}_m + n_{d,mk} \right). \tag{7}$$

Table I
THE OPTIMAL STEP-SIZE AND DISTORTION POWER OF A UNIFORM QUANTIZER WITH BUSSGANG DECOMPOSITION AND UNIT VARIANCE INPUT SIGNAL [30].

α	Δ_{opt}	$p_{\tilde{n}_d} = \tilde{b} - \tilde{a}^2 = \sigma_{\tilde{e}}^2$	$\tilde{a}$
1	1.596	0.2313	0.6366
2	0.9957	0.10472	0.88115
3	0.586	0.036037	0.96256
4	0.3352	0.011409	0.98845
5	0.1881	0.003482	0.996505
6	0.1041	0.0010389	0.99896

Collecting all the receiver filter coefficients $u_{mk}, \forall m$, corresponding to the kth user, we define $\mathbf{u}_k = [u_{1k}, u_{2k}, \cdots, u_{Mk}]^T$. without loss of generality, it is assumed that $||\mathbf{u}_k|| = 1$.

III. PERFORMANCE ANALYSIS

In this section, we derive the spectral efficiency for the considered system model by following a similar approach in [3]. Note that the main difference between the proposed approach and the scheme in [3] is the new set of receiver coefficients which are introduced at the CPU to improve the spectral efficiency. The benefits of the proposed approach in terms of the spectral efficiency is demonstrated through numerical results in Section V. In deriving the spectral efficiency of each user, it is assumed that the CPU exploits only the knowledge of channel statistics between the users and APs in detecting data from the received signal in (7). The aggregated received signal in (7) can be written as

$$r_k = \tilde{a}\underbrace{\sqrt{\rho}\mathbb{E}\left\{\sum_{m=1}^{M} u_{mk}\hat{\mathbf{g}}_{mk}^H \mathbf{g}_{mk}\sqrt{q_k}\right\}}_{\text{DS}_k} s_k + \tilde{a}\underbrace{\sqrt{\rho}\left(\sum_{m=1}^{M} u_{mk}\hat{\mathbf{g}}_{mk}^H \mathbf{g}_{mk}\sqrt{q_k} - \mathbb{E}\left\{\sum_{m=1}^{M} u_{mk}\hat{\mathbf{g}}_{mk}^H \mathbf{g}_{mk}\sqrt{q_k}\right\}\right)}_{\text{BU}_k} s_k$$
$$+ \tilde{a}\sum_{k'\neq k}^{K}\underbrace{\sqrt{\rho}\sum_{m=1}^{M} u_{mk}\hat{\mathbf{g}}_{mk}^H \mathbf{g}_{mk'}\sqrt{q_{k'}}}_{\text{IUI}_{kk'}} s_{k'} + \tilde{a}\underbrace{\sum_{m=1}^{M} u_{mk}\hat{\mathbf{g}}_{mk}^H \mathbf{n}_m}_{\text{TN}_k} + \underbrace{\sum_{m=1}^{M} u_{mk} n_{d,mk}}_{\text{TQD}_k}, \tag{8}$$

where DS_k, BU_k and IUI_k denote the desired signal (DS), beamforming uncertainty (BU) for the kth user, and the inter-user-interference (IUI) caused by the k'th user, respectively. In addition, TN_k accounts for the total noise (TN) following the MRC detection, and finally TQD_k refers to the total quantization distortion (TQD) at the kth user. The elements of quantization distortion are i.i.d. RVs [34]. Moreover, if the probability density function of the input of the quantizer is even and we use a symmetrical quantizer, the quantization noise has zero mean [35]–[37]. In addition, note that using Bussgang decomposition the elements of the quantization distortion are uncorrelated with the input of the quantizer [24], i.e.,

$$\mathbb{E}\left\{\left(\hat{\mathbf{g}}_{mk}^H \mathbf{y}_m\right)^H n_{d,mk}\right\} = 0. \tag{9}$$

Exploiting (9), we have

$$\mathbb{E}\left\{(\mathrm{DS}_k.s_k + \mathrm{BU}_k.s_k) \times \mathrm{TQD}_k\right\} = 0. \tag{10}$$

Hence, exploiting the analysis in [3], it can be shown that terms $\mathrm{DS}_k.s_k$, $\mathrm{BU}_k.s_k$, $\mathrm{IUI}_{kk'}.s_{k'}$, TN_k and TQD_k are mutually uncorrelated. Using the fact that uncorrelated Gaussian noise introduces the worst case, we obtain the corresponding spectral efficiency (in bit/s/Hz) of the received signal in (8) as follows:

$$S_k = \left(1 - \frac{\tau_p}{\tau_c}\right) \log_2\left(1 + \mathrm{SINR}_k\right) = \left(1-\frac{\tau_p}{\tau_c}\right)\log_2\left(1+\frac{|\mathrm{DS}_k|^2}{\mathbb{E}\left\{|\mathrm{BU}_k|^2\right\}+\sum_{k'\neq k}^{K}\mathbb{E}\{|\mathrm{IUI}_{kk'}|^2\} + \mathbb{E}\{|\mathrm{TN}_k|^2\}+\frac{1}{\tilde{a}^2}\mathbb{E}\{|\mathrm{TQD}_k|^2\}}\right). \tag{11}$$

where SINR_k refers to the signal-to-interference-plus-noise ratio (SINR) of the *k*th user and its closed-form expression is provided in the following theorem.[3]

Theorem 1. *By employing MRC detection at the APs, the achievable uplink SINR of the kth user in the cell-free Massive MIMO system with K randomly distributed single-antenna users and M APs, each is equipped with N antennas, is given by*

$$\mathit{SINR}_k = \frac{N^2\mathbf{u}_k^H\left(q_k\boldsymbol{\Gamma}_k\boldsymbol{\Gamma}_k^H\right)\mathbf{u}_k}{\mathbf{u}_k^H\left(N^2\sum\limits_{k'\neq k}^{K}q_{k'}|\boldsymbol{\phi}_k^H\boldsymbol{\phi}_{k'}|^2\boldsymbol{\Delta}_{kk'}\boldsymbol{\Delta}_{kk'}^H+N^2\sum\limits_{k'=1}^{K}q_{k'}|\boldsymbol{\phi}_k^H\boldsymbol{\phi}_{k'}|^2\boldsymbol{\Lambda}_{k'}+N\sum\limits_{k'=1}^{K}q_{k'}\mathbf{D}_{kk'}+\frac{N}{\rho}\mathbf{R}_k\right)\mathbf{u}_k}, \tag{12}$$

where

$$\boldsymbol{\Gamma}_k = [\gamma_{1k}, \gamma_{2k}, \cdots, \gamma_{Mk}]^T,\ \boldsymbol{\Delta}_{kk'} = \left[\frac{\gamma_{1k}\beta_{1k'}}{\beta_{1k}}, \frac{\gamma_{2k}\beta_{2k'}}{\beta_{2k}}, \cdots, \frac{\gamma_{Mk}\beta_{Mk'}}{\beta_{Mk}}\right]^T, \tag{13a}$$

$$\boldsymbol{\Lambda}_{k'} = \frac{\sigma_{\tilde{e}}^2}{\tilde{a}^2}\ diag\left[\gamma_{1k'}^2,\cdots,\gamma_{Mk'}^2\right],\ \mathbf{D}_{kk'} = \left(\frac{\sigma_{\tilde{e}}^2}{\tilde{a}^2}+1\right) diag\left[\beta_{1k'}\gamma_{1k},\cdots,\beta_{Mk'}\gamma_{Mk}\right], \tag{13b}$$

$$\mathbf{R}_k = \left(\frac{\sigma_{\tilde{e}}^2}{\tilde{a}^2}+1\right) diag\left[\gamma_{1k}, \cdots, \gamma_{Mk}\right], \tag{13c}$$

and where $\gamma_{mk} = \sqrt{\tau_p p_p}\beta_{mk}c_{mk}$.

Proof: Please refer to Appendix A. ■

Finally, the sum spectral efficiency is given by

$$S\left(q_k, \mathbf{u}_k, \alpha\right) = \sum_{k=1}^{K} S_k\left(q_k, \mathbf{u}_k, \alpha\right). \tag{14}$$

[3]Note that the expectations are taken over small-scale fading and noise in (8)-(11).

IV. Total Energy Efficiency Model

A. Power Consumption Model

The total power consumption can be defined as follows [38]:

$$P_{\text{total}} = P_{\text{TX}} + P_{\text{CP}}, \tag{15}$$

where P_{TX} is the uplink power amplifiers (PAs) due to transmit power at the users and PA dissipation [38], and P_{CP} refers to the circuit power (CP) consumption. The power consumption P_{TX} is given by

$$P_{\text{TX}} = \frac{1}{\zeta}\rho N_0 \sum_{k=1}^{K} q_k, \tag{16}$$

where ζ is the PA efficiency at each user. The power consumption P_{CP} is obtained as

$$P_{\text{CP}} = MP_{\text{fix}} + KP_{\text{U}} + \sum_{m=1}^{M} P_{\text{bh},m}, \tag{17}$$

where P_{fix} is a fixed power consumption (including control signals and backhaul) at each AP, P_U denotes the required power to run circuit components at each user and finally, backhaul power consumption from the mth AP to the CPU is obtained as follows [25], [39]–[41]:

$$P_{\text{bh},m} = P_{\text{BT}} \ \frac{R_{\text{bh},m}}{C_{\text{bh},m}}, \tag{18}$$

where P_{BT} is the total power required for backhaul traffic (BT) at full capacity, $C_{\text{bh},m}$ is the capacity of the backhaul link between the mth AP and the CPU, and finally $R_{\text{bh},m}$ is the actual backhaul rate between the mth AP and the CPU and is given by [25], [39]–[41]

$$R_{\text{bh},m} = \frac{2 \ K \ \tau_f \ \alpha_m}{T_c}, \tag{19}$$

where α_m denotes the number of quantization bits at each AP and for simplicity we consider the same number of bits at all APs, drop the index m and use α as the number of quantization bits. Moreover, τ_f introduces the length of the uplink data (in symbols) and is given by $\tau_f = \tau_c - \tau_p$, where τ_c denotes the number of samples for each coherence interval, τ_p represents the length of pilot sequence, and finally T_c refers to coherence time in seconds. Note that in (19) α is related to the total uplink spectral efficiency, since it will affect the TQD term and hence the total spectral efficiency in (11).

B. Total Energy Efficiency

In this section, we formulate the total energy efficiency of cell-free Massive MIMO uplink. The total energy efficiency is obtained by dividing the sum throughput (bit/s) by the total consumed power (W) which is given by

$$E_e\left(q_k, \mathbf{u}_k, \alpha\right) = \frac{B \ . \ S\left(q_k, \mathbf{u}_k, \alpha\right)}{P_{\text{total}}} \ \left(\frac{\text{bit}}{\text{Joule}}\right), \tag{20}$$

where B is the bandwidth.

V. Total Energy Efficiency Maximization

In this section, we propose a total energy efficiency maximization problem in cell-free Massive MIMO, where we design the number of quantization bits α, the receiver filter coefficients $\mathbf{u}_k$ and the power coefficients q_k to maximize the total energy efficiency under per-user power and per-user spectral efficiency constraints. Hence, the total energy efficiency maximization can be modeled as follows:

$$P_1: \quad \max_{q_k, \mathbf{u}_k, \alpha} \quad E_e\left(q_k, \mathbf{u}_k, \alpha\right) \tag{21a}$$

$$\text{s.t.} \quad S_k\left(q_k, \mathbf{u}_k\right) \geq S_k^{(\text{r})}, \quad \forall k, \tag{21b}$$

$$||\mathbf{u}_k|| = 1, \ \forall k, \tag{21c}$$

$$0 \leq q_k \leq p_{\text{max}}^{(k)}, \quad \forall k, \tag{21d}$$

$$R_{bh,m} \leq C_{\text{bh},m}, \quad \forall m, \tag{21e}$$

where $S_k^{(\text{r})}$ is the required spectral efficiency of the kth user, $p_{\text{max}}^{(k)}$ and $C_{\text{bh},m}$ refer to the maximum transmit power available at user k and the capacity of backhaul link between the mth AP and the CPU, respectively. Assuming the same amount of backhaul capacity between all APs and the CPU, we drop the index m, and use C_{bh} for simplicity. Using the analysis in Section IV, Problem P_1 can be written as

$$P_2: \max_{q_k, \mathbf{u}_k, \alpha} \ \frac{B \ . \ S\left(q_k, \mathbf{u}_k, \alpha\right)}{\frac{1}{\zeta}\rho N_0 \sum_{k=1}^{K} q_k + M P_{\text{fix}} + K P_{\text{U}} + P_{\text{BT}} \frac{2 \ K \ \tau_f \ \alpha}{T_c} \frac{P_{\text{BT}}}{C_{\text{bh}}}} \tag{22a}$$

$$\text{s.t.} \quad S_k\left(q_k, \mathbf{u}_k, \alpha\right) \geq S_k^{(\text{r})}, \quad \forall k, \tag{22b}$$

$$||\mathbf{u}_k|| = 1, \ \forall k, \tag{22c}$$

$$0 \leq q_k \leq p_{\text{max}}^{(k)}, \quad \forall k, \tag{22d}$$

$$R_{bh} \leq C_{\text{bh}}, \quad \forall m. \tag{22e}$$

Problem P_2 contains one discrete variable (the number of quantization bits). Note that the number of quantization bits, α, can take only discrete values. Hence, we can formulate the problem for fixed values of the number of quantization bits α, and we investigate the optimal values of α numerically. As a result, for a given α, the total energy efficiency maximization problem can be re-formulated as follows:

$$P_3: \max_{q_k, \mathbf{u}_k} \ \frac{B \ . \ S\left(q_k, \mathbf{u}_k, \alpha\right)}{\frac{1}{\zeta}\rho N_0 \sum_{k=1}^{K} q_k + M P_{\text{fix}} + K P_{\text{U}} + P_{\text{BT}} \frac{2 \ K \ \tau_f \ \alpha}{T_c} \frac{P_{\text{BT}}}{C_{\text{bh}}}} \tag{23a}$$

$$\text{s.t.} \qquad S_k\left(q_k, \mathbf{u}_k, \alpha\right) \geq S_k^{(\text{r})}, \quad \forall k, \tag{23b}$$

$$||\mathbf{u}_k|| = 1, \ \forall k, \tag{23c}$$

$$0 \leq q_k \leq p_{\max}^{(k)}, \quad \forall k. \tag{23d}$$

We then reformulate Problem P_3 into the following problem:

$$P_4: \max_{q_k, \mathbf{u}_k, \nu} \ \frac{B \ . \ S\left(q_k, \mathbf{u}_k, \alpha\right)}{\frac{1}{\zeta}\rho N_0 \nu \sum_{k=1}^{K} p_{\max}^{(k)} + M P_{\text{fix}} + K P_{\text{U}} + P_{\text{BT}} \frac{2 \ K \ \tau_f \ \alpha}{T_c} \frac{P_{\text{BT}}}{C_{\text{bh}}}} \tag{24a}$$

$$\text{s.t.} \qquad S_k\left(q_k, \mathbf{u}_k, \alpha\right) \geq S_k^{(\text{r})}, \quad \forall k, \tag{24b}$$

$$||\mathbf{u}_k|| = 1, \ \forall k, \tag{24c}$$

$$0 \leq q_k \leq p_{\max}^{(k)}, \forall k, \tag{24d}$$

$$\sum_{k=1}^{K} q_k \leq \nu \sum_{k=1}^{K} p_{\max}^{(k)}, \tag{24e}$$

$$\nu^* \leq \nu \leq 1, \tag{24f}$$

where ν is a auxiliary variable and ν^* and is obtained through the following remark.

Remark 2. *Based on the analysis in [42], [43], the slack variable ν^* is obtained by solving a power minimization problem subject to the same per-user power constraints in (24d) and throughput requirement constraints in (24b). For details, please refer to Appendix B.* ■

Theorem 2. *The optimal solution of Problem P_3 and problem P_4 are equal.*

Proof: The proof of Theorem 2 follows the same approach in the proof of [42, Theorem 1]. Let us assume $\{\mathbf{U}^{\text{opt}}, \mathbf{q}^{\text{opt}}\}$ and $\{\dot{\mathbf{U}}^{\text{opt}}, \dot{\mathbf{q}}^{\text{opt}}, \dot{\nu}\}$ are the optimal solution of Problems P_3 and P_4, respectively. It is easy to show that $\sum_{k=1}^{K} \dot{q}_k = \dot{\nu} \sum_{k=1}^{K} p_{\max}^{(k)}$. Moreover, based on [42], it is clear that $\dot{\mathbf{U}}^{\text{opt}}$ and $\dot{\mathbf{q}}^{\text{opt}}$ provide a feasible solution to Problem P_3. Exploiting the per-user power constraints, using $\nu = \frac{1}{\sum_{k=1}^{K} p_{\max}^{(k)}} \sum_{k=1}^{K} q_k$ and $0 \leq \nu \leq 1$, and by considering the throughput requirement constraints, one can conclude that $\{\mathbf{U}^{\text{opt}}, \mathbf{q}^{\text{opt}}\}$ provide a feasible solution to Problem

P_4. Through these two facts, it is not difficult to show that the optimal solutions of Problems P_3 and P_4 are equal, which completes the proof of Theorem 2. ■

Hence, we can convert the original total energy efficiency maximization problem into a total energy efficiency maximization problem with per-user power constraints, throughput requirement constraints and the new total power constraint. Next, Problem P_4 is iteratively solved by performing a one-dimensional search over the variable $\nu^* \leq \nu \leq 1$ [42]. Therefore, for a given ν, the denominator of the objective function of Problem P_4 is a constant, which enables us to define the following equivalent optimization problem:

$$P_5: \max_{q_k, \mathbf{u}_k} \quad S\left(q_k, \mathbf{u}_k, \alpha\right) \tag{25a}$$

$$\text{s.t.} \quad S_k\left(q_k, \mathbf{u}_k, \alpha\right) \geq S_k^{(\mathrm{r})}, \quad \forall k, \tag{25b}$$

$$||\mathbf{u}_k|| = 1, \ \forall k, \tag{25c}$$

$$0 \leq q_k \leq p_{\max}^{(k)}, \forall k, \tag{25d}$$

$$\sum_{k=1}^{K} q_k \leq \nu \sum_{k=1}^{K} p_{\max}^{(k)}. \tag{25e}$$

Problem P_5 is not convex in terms of $\mathbf{u}_k$ and power allocation $q_k, \ \forall k$. Therefore, it cannot be directly solved through existing convex optimization software. To tackle this non-convexity issue, we decouple Problem P_5 into two sub-problems: receiver coefficient design (i.e. $\mathbf{u}_k$) and the power allocation problem. The optimal solution for Problem P_5, is obtained through alternately solving these sub-problems, as explained in the following subsections.

A. Receiver Filter Coefficient Design

In this subsection, the problem of designing the receiver filter coefficient vector is considered. We solve the total energy efficiency maximization problem for a given set of power allocations at all users, $q_k, \forall k$, and fixed values for the number of quantization bits, $\alpha_m, \ \forall m$. These coefficients (i.e., $\mathbf{u}_k$, $\forall\ k$) are obtained by independently maximizing the total uplink energy efficiency of the system. Note that the spectral efficiency of the kth user, i.e., $S_k\left(q_k, \mathbf{u}_k, \alpha\right)$, is a function of only $\mathbf{u}_k$ (it does not depend on $\mathbf{u}_{k'}$, where $k' \neq k$), and hence, the optimal receiver filter coefficients can be determined by solving the following optimization problem:

$$P_6: \max_{\mathbf{u}_k} \quad S_k\left(q_k, \mathbf{u}_k, \alpha\right) \tag{26a}$$

$$\text{s.t.} \quad S_k\left(q_k, \mathbf{u}_k, \alpha\right) \geq S_k^{(\mathrm{r})}, \quad \forall k, \tag{26b}$$

$$||\mathbf{u}_k|| = 1, \ \forall k. \tag{26c}$$

Note that the satisfaction of constraints in (26b) will be ensured in the power allocation problem. Hence, we drop constraint (26b) and Problem P_6 can be reformulated as:

$$P_7: \max_{\mathbf{u}_k} \frac{N^2 \mathbf{u}_k^H \left(q_k \mathbf{\Gamma}_k \mathbf{\Gamma}_k^H\right) \mathbf{u}_k}{\mathbf{u}_k^H \left(N^2 \sum\limits_{k' \neq k}^{K} q_{k'} |\boldsymbol{\phi}_k^H \boldsymbol{\phi}_{k'}|^2 \mathbf{\Delta}_{kk'} \mathbf{\Delta}_{kk'}^H + N^2 \sum\limits_{k'=1}^{K} q_{k'} |\boldsymbol{\phi}_k^H \boldsymbol{\phi}_{k'}|^2 \mathbf{\Lambda}_{k'} + N \sum\limits_{k'=1}^{K} q_{k'} \mathbf{D}_{kk'} + \frac{N}{\rho} \mathbf{R}_k\right) \mathbf{u}_k} \tag{27a}$$

$$\text{s.t.} \quad ||\mathbf{u}_k|| = 1, \ \forall k. \tag{27b}$$

Problem P_7 is a generalized eigenvalue problem [5], [44]–[46], where the optimal solutions can be obtained by determining the generalized eigen vector of the matrix pair $\mathbf{A}_k = N^2 q_k \mathbf{\Gamma}_k \mathbf{\Gamma}_k^H$ and $\mathbf{B}_k = N^2 \sum_{k' \neq k}^{K} q_{k'} |\boldsymbol{\phi}_k^H \boldsymbol{\phi}_{k'}|^2 \mathbf{\Delta}_{kk'} \mathbf{\Delta}_{kk'}^H + N^2 \sum_{k'=1}^{K} q_{k'} |\boldsymbol{\phi}_k^H \boldsymbol{\phi}_{k'}|^2 \mathbf{\Lambda}_{k'} + N \sum_{k'=1}^{K} q_{k'} \mathbf{D}_{kk'} + \frac{N}{\rho} \mathbf{R}_k$ corresponding to the maximum generalized eigenvalue.

B. Power Allocation

In this subsection, we solve the power allocation problem for a given set of fixed receiver filter coefficients, $\mathbf{u}_k$, $\forall\ k$, and fixed values of quantization levels, Q_m, $\forall m$. The optimal transmit power can be determined by solving the following total spectral efficiency maximization problem:

$$P_8: \max_{q_k} \quad S\left(q_k, \mathbf{u}_k, \alpha\right) \tag{28a}$$

$$\text{s.t.} \quad S_k\left(q_k, \mathbf{u}_k, \alpha\right) \geq S_k^{(\mathrm{r})}, \quad \forall k, \tag{28b}$$

$$0 \leq q_k \leq p_{\max}^{(k)}, \quad \forall k, \tag{28c}$$

$$\sum_{k=1}^{K} q_k \leq \nu \sum_{k=1}^{K} p_{\max}^{(k)}. \tag{28d}$$

Problem P_8 can be reformulated as follows:

$$P_9: \min_{q_k} \quad \prod_{k=1}^{K} \left(1 + \text{SINR}_k\left(q_k, \mathbf{u}_k, \alpha\right)\right)^{-1} \tag{29a}$$

$$\text{s.t.} \quad S_k\left(q_k, \mathbf{u}_k, \alpha\right) \geq S_k^{(\mathrm{r})}, \quad \forall k, \tag{29b}$$

$$0 \leq q_k \leq p_{\max}^{(k)}, \quad \forall k, \tag{29c}$$

$$\sum_{k=1}^{K} q_k \leq \nu \sum_{k=1}^{K} p_{\max}^{(k)}. \tag{29d}$$

Problem P_9 is generally a non-convex problem, however, it can be reformulated as a standard GP problem [47]. We first rewrite Problem P_9 as follows:

$$P_{10}: \min_{q_k, t_k} \quad \prod_{k=1}^{K} (1+t_k)^{-1} \tag{30a}$$

$$\text{s.t.} \quad S_k\left(q_k, \mathbf{u}_k, \alpha\right) \geq S_k^{(\mathrm{r})}, \quad \forall k, \tag{30b}$$

$$0 \leq q_k \leq p_{\max}^{(k)}, \forall k, \tag{30c}$$

$$\mathrm{SINR}_k \geq t_k, \forall k, \tag{30d}$$

$$\sum_{k=1}^{K} q_k \leq \nu \sum_{k=1}^{K} p_{\max}^{(k)}, \tag{30e}$$

where $t_k, \forall k$ refers to the slack variables. Problem (30) is a non-convex signomial problem. However, in Appendix C, we will show that all constraints in (30) can be reformulated into posynomial functions. Hence, if the objective function in (30) can be reformulated into a posynomial function, problem (30) is a standard GP and has an optimal solution [47]. This motivates us to propose two schemes to transform Problem (30) into a standard GP.

1) Efficient Power Allocation Scheme: We use the SCA scheme proposed in [48] to convert Problem (30) into a standard GP. This scheme is referred to as the "inner approximation algorithm for non-convex problems" in [48], and introduces an efficient solution for the original problem [42], [48]. Based on the analysis in [48], it is possible to search for a local optimum through solving a sequence of GPs which locally approximate the original optimization problem. This scheme is called the "inner approximation algorithm for non-convex problems" in [48]. This scheme provides an efficient solution for the original problem [42], [48]. Next, the following lemma using SCA is required [42, Lemma 1]:

Lemma 1. *Function $\Theta(x) = \kappa t^{\xi}$ can be used to approximate function $\Pi(x) = 1 + t$, near the point $\hat{t}$. The best monomial local approximation is obtained by the following parameters:*

$$\xi = \frac{\hat{t}}{1+\hat{t}}, \ \kappa = \frac{1+\hat{t}}{\hat{t}^{\xi}}, \tag{31}$$

where $\Theta(t) \leq \Pi(t)$, $\forall t > 0$.

Using the local approximation in Lemma 1, we can tackle the non-convexity of Problem P_{10}, which enables us to reformulate Problem P_{10} as follows:

Algorithm 1 Proposed algorithm to solve Problem P_5

1. Initialize $\mathbf{q}^{(0)}$, $\mathbf{U}^{(0)}$. Calculate the uplink $\text{SINR}_k^{(0)}$, $t_0^{(0)}$ and $S_k^{(r)}$ using $\mathbf{q}^{(0)}$ and $\mathbf{U}^{(0)}$, and set the initial SINR guess and initial auxiliary variables as $\hat{t}_k = \text{SINR}_k^{(0)}, \forall k$, and $t_k^{(0)} = \text{SINR}_k^{(0)}, \forall k$, respectively.
2. Set $\mathbf{q}^{(*)} = 0$, $t_k^{(*)} = t_k^{(0)}$, $\mathbf{U}^{(*)} = \mathbf{U}^{(0)}$, and $\tilde{E}_{e,k}^{(*)} = 0, \forall k$.
3. Calculate the constants ξ and κ using (31), and solve problem P_{11} with $t_k^{(*)}$ and $\mathbf{U}^{(*)}$, and find $\mathbf{q}^{(**)}$ and calculate $t_0^{(**)}$ and $t_k^{(**)}$.
4. If $\left|t_k^{(**)} - t_k^{(*)}\right| \leq \epsilon_1$, then set $t_k^{(**)} = t_k^{(*)}$ and $\mathbf{q}^{(**)} = \mathbf{q}^{(*)}$ and go to step 8, otherwise, $t_k^{(*)} = t_k^{(**)}$ and go to step 3.
5. Solve the generalized eigenvalue Problem P_7 using $\mathbf{q}^{(*)}$ and calculate $\mathbf{U}$. Next, let $\mathbf{U}^{(**)} = \mathbf{U}$.
6. Compute the objective value of Problem P_{11} with $\mathbf{U}^{(**)}$ and $\mathbf{q}^{(*)}$ and call it $\tilde{E}_{e,k}^{(**)}, \forall k$.
7. If $\left|\tilde{E}_{e,k}^{(**)} - \tilde{E}_{,k} e^{(*)}\right| \leq \epsilon_2, \forall k$, then $\mathbf{U}^{(*)} = \mathbf{U}^{(**)}$ and go to step 8, otherwise, go to step 3.
8. If the stop criteria is satisfied stop, otherwise, go to step 3.

$$P_{11}: \min_{q_k, t_k} \quad \left(\prod_{k=1}^{K} t_k^{-\frac{\hat{t}_k}{1+\hat{t}_k}}\right) \tag{32a}$$

$$\text{s.t.} \quad S_k\left(q_k, \mathbf{u}_k, \alpha\right) \geq S_k^{(\text{r})}, \quad \forall k, \tag{32b}$$

$$0 \leq q_k \leq p_{\text{max}}^{(k)}, \forall k, \tag{32c}$$

$$\text{SINR}_k \geq t_k, \forall k, \tag{32d}$$

$$\sum_{k=1}^{K} q_k \leq \nu \sum_{k=1}^{K} p_{\text{max}}^{(k)}, \tag{32e}$$

$$\left((1-\delta)\hat{t}_k\right) \leq t_k \leq \left((1-\delta)\hat{t}_k\right), \forall k, \tag{32f}$$

where δ is a constant value to control the approximation accuracy [42].

Proposition 1. *Problem P_{11} can be formulated into a standard GP.*

Proof: Please refer to Appendix C. ■

Therefore, Problem P_{11} is efficiently solved through existing convex optimization software. Based on these two sub-problems (P_7 and P_{11}), an iterative algorithm has been developed by alternately solving both sub-problems at each iteration. The proposed algorithm is summarized in Algorithm 1, where ϵ_1 and ϵ_2 are small values, and we set $\epsilon_1 = \epsilon_2 = 0.01$.

Algorithm 2 Proposed sub-optimal algorithm to solve Problem P_5

1. Initialize $\mathbf{q}^{(0)}$, $i=1$.
2. Repeat steps 3-5 until $\left|\tilde{\tilde{E}}_{e,k}^{(i+1)}-\tilde{\tilde{E}}_{e,k}^{(i)}\right|\leq\epsilon_3,\forall k$, where $\tilde{\tilde{E}}_{e,k}$ is the objective value of Problem P_{10}.
3. $i=i+1$.
4. Set $\mathbf{q}^{(i)}=\mathbf{q}^{(i-1)}$ and determine the optimal receiver coefficients $\mathbf{U}^{(i)}$ through solving the generalized eigenvalue Problem P_7.
5. Compute $\mathbf{q}^{(i+1)}$ through solving Problem P_{12}.

2) Sub-Optimal Power Allocation Scheme: In this section, we present a heuristic solution to tackle the non-convexity issue of Problem P_{10}. Exploiting the analysis in [49], we propose to reformulate the energy efficiency maximization Problem P_8 as follows:

$$P_{12}:\min_{q_k,t_k}\quad\prod_{k=1}^{K}t_k^{-1} \tag{33a}$$

$$\text{s.t.}\quad S_k\left(q_k,\mathbf{u}_k,\alpha\right)\geq S_k^{(\mathrm{r})},\quad\forall k, \tag{33b}$$

$$0\leq q_k\leq p_{\max}^{(k)},\forall k, \tag{33c}$$

$$\mathrm{SINR}_k\geq t_k,\forall k, \tag{33d}$$

$$\sum_{k=1}^{K}q_k\leq\nu\sum_{k=1}^{K}p_{\max}^{(k)}. \tag{33e}$$

Proposition 2. *Problem P_{12} can be formulated into a standard GP.*

Proof: The objective function in (30a) and the power constraint in (30e) are posynomial functions. The spectral efficiency constraint in (30b) and the SINR constraint in (30d) can be rewritten into the posynomial functions similar to (60) and (62), which completes the proof. ■

Hence, existing convex optimization software can be used to solve problem P_{12}. As in the previous section, here we propose an iterative algorithm to iteratively solve sub-problems P_7 and P_{12}. Finally, Algorithm 2 summarizes the proposed scheme.

C. Convergence

In this section, the convergence analysis of the proposed Algorithms 1 and 2 are provided. Two sub-problems are alternately solved to determine the solution to Problem P_2. At each iteration, one of the design parameters is determined by solving the corresponding sub-problem while other design variables are kept fixed. Note that each sub-problem provides an optimal solution

Table II
COMPUTATIONAL COMPLEXITY OF DIFFERENT PROBLEMS

Problem	Required arithmetic operations
Problem P_7	$\frac{14}{3}KM^3$
Problem P_{11}	$n_{\text{iter}} \times \mathcal{O}\left((4K-1)^{\frac{1}{2}}\left(24K^3-20K^2+8K-1\right)\right)$
Problem P_{12}	$\mathcal{O}\left((4K-1)^{\frac{1}{2}}\left(24K^3-20K^2+8K-1\right)\right)$

for the other given design variables. At the nth iteration, the receiver filter coefficients $\mathbf{u}_k^{(n)},\ \forall k$ are determined for a given power allocation $\mathbf{q}^{(n)}$ and similarly, the power allocation $\mathbf{q}^{(n+1)}$ is updated for a given set of receiver filter coefficients $\mathbf{u}_k^{(n)},\ \forall k$. The optimal power allocation $\mathbf{q}^{(n+1)}$ obtained for a given $\mathbf{u}_k^{(n)}$ achieves an uplink spectral efficiency greater than or equal to that of the previous iteration. In addition, the power allocation $\mathbf{q}^{(n)}$ is also a feasible solution in determining $\mathbf{q}^{(n+1)}$ as the receiver filter coefficients $\mathbf{u}_k^{(n+1)},\ \forall k$ are determined for a given $\mathbf{q}^{(n)}$. This reveals that the achieved uplink spectral efficiency monotonically increases with each iteration, which can also be observed from the numerical results presented in Figs. 3a, 3b and 3c. As the achievable uplink energy efficiency is upper bounded by a certain value for a given set of per-user power and spectral efficiency constraints, the proposed algorithms converges to a particular solution. Note that to the best of our knowledge and referring to [50], [51] this is a common way to show the convergence.

D. Complexity analysis

Here, we provide the computational complexity analysis for the proposed Algorithms 1 and 2, which solve a generalized eigenvalue problem P_7 and a GP (convex optimization problem) given by P_{11} and P_{12}, respectively, at each iteration. For the receiver filter coefficient design in P_7, an eigenvalue solver requires $\frac{14}{3}KM^3$ flops for K users using the QR algorithm [52].

Proposition 3. *Problem P_{11}, can be solved with complexity equivalent to $n_{iter} \times \mathcal{O}\left((4K-1)^{\frac{1}{2}}\left(24K^3-20K^2+8K-1\right)\right)$, where n_{iter} refers to the number of iterations in P_{11} which depends on δ in (32f). Note that the term $\mathcal{O}$ means there is an unknown factor. Moreover, it can be shown that Problem P_{12} can be solved with a complexity of $\mathcal{O}\left((4K-1)^{\frac{1}{2}}\left(24K^3-20K^2+8K-1\right)\right)$.*

Proof: Please refer to Appendix D. ■

The number of arithmetic operations required for Algorithms 1 and 2 are provided in Table II.

VI. User Assignment

Let τ_f be the length of the uplink payload data transmission for each coherence interval, i.e., $\tau_f = \tau_c - \tau_p$, where τ_c denotes the number of samples for each coherence interval and τ_p represents the length of pilot sequence. Note that we need $2\alpha_m \times (K\tau_f)$ bits for each AP during each coherence interval. Hence, the total backhaul capacity required between the mth AP and the CPU for all schemes is defined as

$$C_m = \frac{2\left(K\tau_f\right)\alpha_m}{T_c}, \tag{34}$$

where T_c (in sec.) refers to coherence time. Exploiting (34), it is obvious that the total backhaul capacity required between the mth AP and the CPU increases linearly with the total number of users served by the mth AP. This motivates the need to pick a proper set of active users for each AP. Using (34), we have

$$\alpha_m \times K_m \leq \frac{C_{\text{bh}} T_c}{2\tau_f}, \tag{35}$$

where K_m denotes the size of the set of active users for the mth AP. From (35), it can be seen that decreasing the size of the set of active users allows for a larger number of quantization levels. Motivated by this fact, and to exploit the capacity of backhaul links more efficiently, we investigate all possible combinations of α_m and K_m. First, for a fixed value of α_m, we find an upper bound on the size of the set of active users for each AP. In the next step, we propose for all APs that the users are sorted according to $\beta_{mk},\ \forall k$, and find the K_m users which have the highest values of β_{mk} among all users. If a user is not selected by any AP, we propose to find the AP which has the best link to this user ($\pi(j) = \underset{m}{\operatorname{argmax}}\, \beta_{mj}$ determines best link to the jth user, i.e., the index of the AP which is closest to the jth user). Note that to consider only the users that have links to other APs, we use $k|\mathcal{S}_k\pi_j \neq \varnothing$, where $\varnothing$ refers to empty set. Then we drop the user which has the lowest $\beta_{mk},\ \forall k$, among the set of active users for that AP, which has links to other APs as well. Finally, we add the user which is not selected by any AP to the set of active users for this AP. We next solve the uplink energy efficiency maximization problem as follows

$$\begin{aligned}
P^{\text{user assignment}}: \quad & \max_{q_k, \mathbf{u}_k, \alpha} \quad E_e\left(q_k, \mathbf{u}_k, \alpha, \tilde{\gamma}_{mk}\right) && \text{(36a)}\\
& \text{s.t.} \quad\ S_k\left(q_k, \mathbf{u}_k, \tilde{\gamma}_{mk}\right) \geq S_k^{(\text{r})}, \quad \forall k, && \text{(36b)}\\
& \qquad\quad\ ||\mathbf{u}_k|| = 1,\ \forall k,\ 0 \leq q_k \leq p_{\max}^{(k)},\ \forall k,\ R_{bh,m} \leq C_{\text{bh},m},\ \forall m, && \text{(36c)}
\end{aligned}$$

where

$$\tilde{\gamma}_{mk} = \begin{cases} \gamma_{mk}, & m \in \mathcal{S}_k \\ 0, & \text{otherwise} \end{cases} \tag{37}$$

where $\mathcal{S}_k$ refers to the set of active APs for the kth user. Finally, note that this reduces the complexity of the optimization problem, as some entries of $\tilde{\gamma}_{mk}$ are zero. Finally, note that we turn off the mth AP, if the set of active users for the mth AP is empty, after performing the user assignment scheme. Hence, we put the number of active APs instead of M. This will reduce the complexity of the proposed scheme.

VII. Numerical Results and Discussion

In this section, we provide numerical numerical results to validate the performance of the proposed scheme. A cell-free Massive MIMO system with M APs and K single-antenna users is considered in a $D \times D$ numerical area, where both APs and users are uniformly distributed at random points. In the following subsections, we define the numerical parameters and then present the corresponding numerical results.

A. Simulation Parameters

The channel coefficients between users and APs are modeled in Section II, where the coefficient β_{mk} is given by [3]

$$\beta_{mk} = \text{PL}_{mk} 10^{\frac{\sigma_{sh}\ z_{mk}}{10}}, \tag{38}$$

where PL_{mk} is the path loss from the kth user to the mth AP and the second term in (38), $10^{\frac{\sigma_{sh} z_{mk}}{10}}$, denotes the shadow fading with standard deviation $\sigma_{sh} = 8$ dB, and $z_{mk} \sim \mathcal{N}(0,1)$. In the simulation, an uncorrelated shadowing model is considered and a three-slope model for the path loss is given by [3]

$$\text{PL}_{mk} = \begin{cases} -L - 35\log_{10}(d_{mk}/1\text{ m}), & d_{mk} > d_1, \\ -L - 15\log_{10}(d_1\ /1\text{ m}) - 20\log_{10}(d_{mk}/1\text{ m}), & d_0 < d_{mk} \leq d_1, \\ -L - 15\log_{10}(d_1/1\text{ m}) - 20\log_{10}(d_0/1\text{ m}), & d_{mk} \leq d_0, \end{cases} \tag{39}$$

and $L = 46.3 + 33.9\log_{10}(f) - 13.82\log_{10}(h_{AP}) - (1.1\log_{10}(f) - 0.7)\, h_k + (1.56\log_{10}(f) - 0.8)$, where f denotes the carrier frequency (in MHz), h_{AP} and h_k represent the AP antenna height (in m) and user height (in m), respectively. The noise power is given by $p_n = \text{BW} \times k_B \times T_0 \times W$, where $\text{BW} = 20$ MHz denotes the bandwidth, $k_B = 1.381 \times 10^{-23}$ represents the Boltzmann constant, and $T_0 = 290$ (K) denotes the noise temperature. Moreover, $W = 9$ dB, and denotes the noise figure. It is assumed that $\bar{p}_p$ and $\bar{\rho}$ denote the power of the pilot sequence and the uplink data powers, respectively, where $p_p = \frac{\bar{p}_p}{p_n}$ and $\rho = \frac{\bar{\rho}}{p_n}$ are normalized transmit SNRs. In

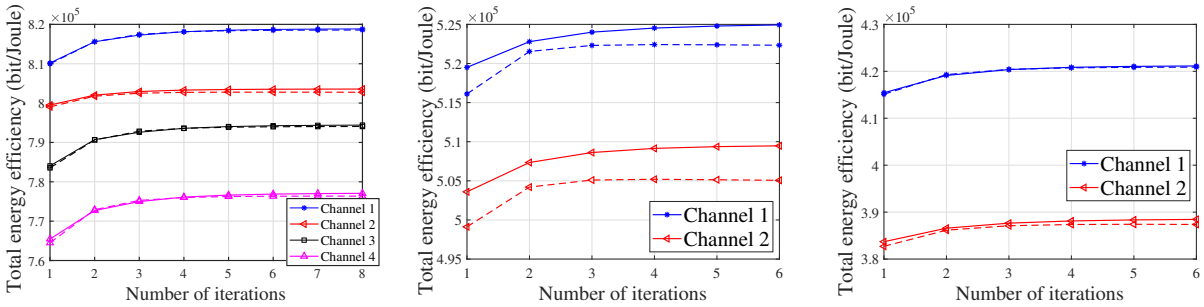

(a) Here $K = 20$, $M = 100$, $N = 1$, $\alpha = 2$, $\tau_p = 20$, and $D = 1$ km. (b) Here $K = 40$, $M = 100$, $N = 1$, $\alpha = 2$, $\tau_p = 20$, and $D = 1$ km. (c) Here $K = 40$, $M = 200$, $N = 1$, $\alpha = 2$, $\tau_p = 20$, and $D = 1$ km

Figure 3. The total energy efficiency of proposed Algorithm 1 (solid curves) and proposed Algorithm 2 (dashed curves) versus number of iterations.

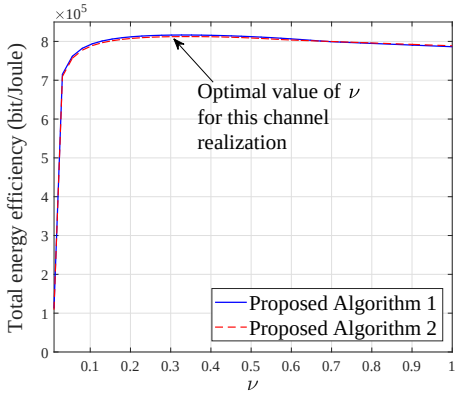

Figure 4. The total energy efficiency of proposed Algorithm 1 and proposed Algorithm 2 versus ν for one channel realization with $K = 20$, $M = 100$, $N = 1$, $\alpha = 2$, $\tau_p = 20$, and $D = 1$ km.

simulations, we set $\bar{p}_p = 200$ mW and $\bar{\rho} = 1$ W. Similar to [3], we assume that the simulation area is wrapped around at the edges which can simulate an area without boundaries. Hence, the square simulation area has eight neighbours. Moreover, we set $\zeta = 0.3$, $P_U = 0.1$ W, $P_{\text{fix}} = .825$ W [25], [38]–[41]. Moreover, hereafter the term "orthogonal pilots" refers to the case where unique orthogonal pilots are assigned to all users, while in "random pilot assignment" each user is randomly assigned a pilot sequence from a set of orthogonal sequences of length τ_p ($< K$), following the approach of [3].

B. Numerical Results

1) Convergence of the Proposed Schemes: In this section, the convergence of the proposed Algorithms 1 and 2 is investigated. Figs. 3a, 3b and 3c present the convergence of the proposed Algorithms 1 and 2 with $M = 100$ and $M = 200$ APs, and $K = 20$ and $K = 40$ users with the length of pilot $\tau_p = 20$. Note that in Figs. 3a, 3b and 3c, the solid and dashed curves represent

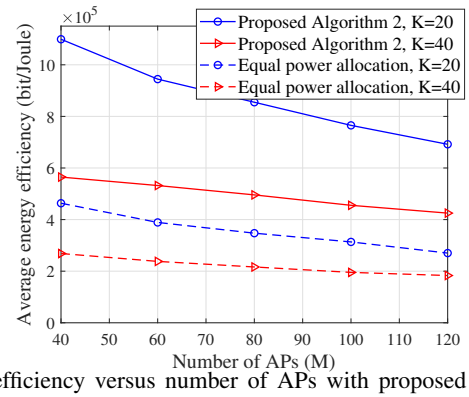

Figure 5. The average total energy efficiency versus number of APs with proposed Algorithm 1 and equal power allocation with $N = 1$, $\alpha = 2$, $\tau_p = 20$, and $D = 1$ km.

the performance of proposed Algorithm 1 and Algorithm 2, respectively. The figures confirm that the proposed Algorithms 1 and 2 converge in a few iterations.

Figs. 3a, 3b and 3c demonstrate that the proposed sub-optimal scheme has a performance fairly close to the performance of the proposed Algorithm 1. As Algorithm 2 has a lower complexity and good performance, in the rest of numerical results, we investigate the performance using only the proposed Algorithm 2.

2) The optimal value of ν: To study the effect of ν in Problem P_5, we solve Problem P_5 with different values of ν and plot the total energy efficiency versus ν in Fig. 4. For this channel realization, for both proposed Algorithms 1 and 2, the optimal value of ν has a range from $0.25 - 0.35$, and we set the optimal value to $\nu^{\text{opt}} = 0.3$.

3) Performance Comparison: Fig. 5 presents the total energy efficiency of the proposed Algorithm 2 and the scheme with the equal power allocation with $M = 100$, $N = 1$, $\alpha = 2$, $\tau_p = 20$, and $D = 1$ km. As seen in Fig. 5, the proposed scheme significantly improves the total energy efficiency of cell-free Massive MIMO compared to equal power allocation scheme (i.e., $q_k = 1, \forall k, \mathbf{u}_k = [1, \cdots, 1], \forall k$).

4) Effect of the Number of Quantization Bits: This section investigates the optimum values of number of quantization bits to maximize the energy efficiency of cell-free Massive MIMO. Increasing the number of quantization bits introduces spectral efficiency improvement whereas it increases the backhaul power consumption from the APs to the CPU. Therefore, there is an optimum value in terms of number of quantization bits to maximize the total energy efficiency of the cell-free Massive MIMO system. The average energy efficiency versus the number of quantization bits is shown in Fig. 6 for the system with $\{K = 40, N = 5, P_{\text{BT}} = 1$ W, $\rho = 3$

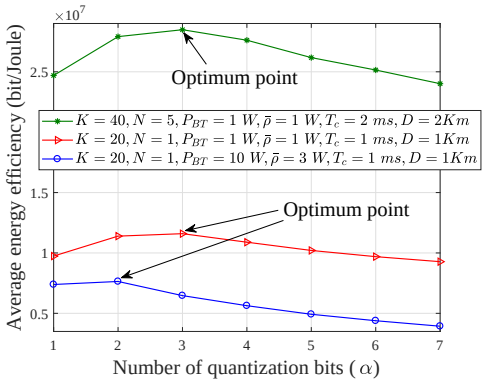

Figure 6. The average total energy efficiency of proposed Algorithm 2 versus number of quantization bits with $K = 20$, $N = 1$, $\tau_p = 20$, and $D = 1$ km.

W, $T_c = 2$ ms, $D = 2$ Km$\}$, $\{K = 20, N = 1, P_{\text{BT}} = 1$ W, $\rho = 1$ W, $T_c = 1$ ms, $D = 1$ Km$\}$, $\{K = 40, N = 5, P_{\text{BT}} = 10$ W, $\rho = 3$ W, $T_c = 1$ ms, $D = 1$ Km$\}$ with orthogonal pilots. Optimally, we need only 2-4 bits to quantize the data.

5) Effect of the Number of Antennas per AP: In this section, the performance of cell-free Massive MIMO is studied with different numbers of antennas per AP. Similar to the methodolgy in [50], we set $MN = 256$ as the total number of service antennas. The average energy efficiency of the system is shown in Fig. 7, for $K = 40$, $\alpha = 4$ bits, and $P_{\text{BT}} = 10$ W. Moreover, we provide numerical results for two cases of orthogonal and random pilot assignment. It can be seen for a fixed total number of service antennas, by reducing the total number of APs, M (which is equivalent to increasing number of antennas per APs, N), the total power consumption will decrease. On the other hand, reducing M results in throughput reduction. As a result, one can find a trade off between M and N. Fig. 7 reveals the optimum values of M and N to have the largest total energy efficiency.

6) Effect of Power of Backhaul Links: Fig. 8 shows the average energy efficiency of the cell-free Massive MIMO system versus the total backhaul traffic power, P_{BT}, for $K = 20$, $N = 1$, $\tau_p = 20$, $D = 1$ km, $C_{bh} = 102.4$ Mbps, and two cases of $M = 60$ and $M = 120$. As the figure demonstrates, the average energy efficiency decreases as the total power for backhaul traffic increases.

7) Energy Efficiency vs Relative Loss in Max-Min Spectral Efficiency: It is interesting to evaluate how much we can gain with the proposed energy efficiency power control by sacrificing the required spectral efficiency. To investigate this, we consider the max-min spectral efficiency problem defined in [53] with a given backhaul rate, which is defined as follows:

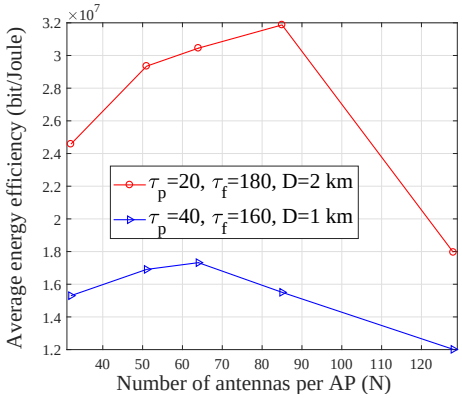

Figure 7. The average total energy efficiency of proposed Algorithm 2 versus the number of antennas per AP with $K = 40$, $MN = 256$, $P_{BT} = 10$ W, $C_{bh} = 100$ Mbps, and $\alpha = 4$ bits.

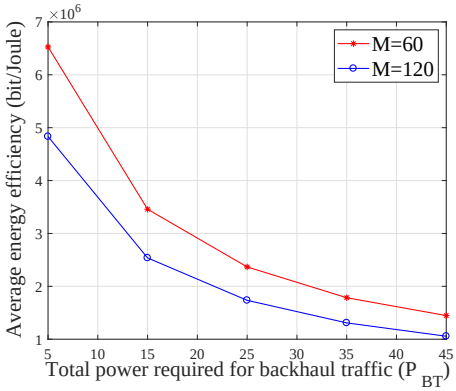

Figure 8. The average total energy efficiency of proposed Algorithm 2 versus number of quantization bits with $K = 20$, $N = 1$, $\tau_p = 20$, $D = 1$ km, $C_{bh} = 102.4$ Mbps, and two cases of $M = 60$ and $M = 120$.

$$P^{\text{max-min}}: \max_{q_k, \mathbf{u}_k} \quad \min_{k=1,\cdots,K} \quad R_k, \tag{40a}$$

$$\text{s.t.} \quad ||\mathbf{u}_k|| = 1, \ \forall k, \tag{40b}$$

$$0 \leq q_k \leq p_{\text{max}}^{(k)}, \quad \forall k. \tag{40c}$$

where R_k refers to the rate of the kth user given in [53]. The details to solve Problem $P^{\text{max-min}}$ are presented in [53]. Next, we define the following optimization problem:

$$P^{\text{sac}}: \max_{q_k, \mathbf{u}_k} \quad E_e\left(q_k, \mathbf{u}_k\right), \tag{41a}$$

$$\text{s.t.} \quad S_k\left(q_k, \mathbf{u}_k\right) \geq \left(\text{th}_{\text{sac}} \times S_k^{(\text{max-min})}\right), \quad \forall k, \tag{41b}$$

$$||\mathbf{u}_k|| = 1, \ \forall k, \ 0 \leq q_k \leq p_{\text{max}}^{(k)}, \quad \forall k, \tag{41c}$$

where $S_k^{(\text{max-min})} = (1 - \frac{\tau_p}{\tau_c}) R_k^{\text{max-min}}$, where $R_k^{\text{max-min}}$ is the optimal solution of Problem $P^{\text{max-min}}$. Fig. 9 presents the average energy efficiency performance of the cell-free Massive MIMO with

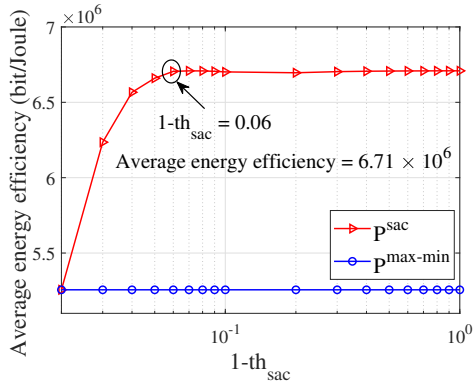

Figure 9. The average energy efficiency of proposed Algorithm 2 versus the sacrifice in max-min spectral efficiency for $K = 15$, $M = 80$, $N = 1$, $\tau_p = 15$, $D = 1$ km, $\alpha = 2$, $P_{\text{BT}} = 1$ W and $C_{bh} = 100$ Mbps.

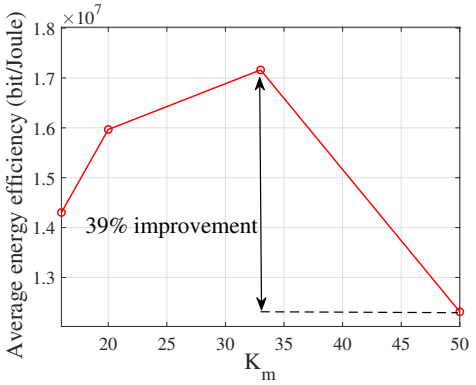

Figure 10. The average energy efficiency of proposed Algorithm 2 versus the total number of active users for each AP with $M = 40$, $N = 4$, $K = 50$, $\tau_p = 30$ and $\alpha_m \times K_m = 100$.

$M = 80$, $K = 15$, $N = 1$, $\alpha = 2$ and orthogonal pilots, obtained by solving Problems $P^{\text{max-min}}$ and P^{sac}. Note that we use the sub-optimal power allocation scheme presented in Subsection V-B2 to solve Problem P^{sac}. The figure shows that by sacrificing 6% of the max-min spectral efficiency (i.e., $1 - \text{th}_{\text{sac}} = 0.06$), one could gain $\frac{6.71\times10^6 - 5.25\times10^6}{5.25\times10^6} = 27.8\%$ improvement in the average energy efficiency of the system.

8) Performance of the Proposed User Assignment Scheme: This subsection investigates the performance of the proposed user assignment scheme. In Fig. 10, the average energy efficiency proposed using Algorithm 2 is presented with $M = 40$, $N = 4$, $K = 50$, and $\tau_p = 30$ versus the total number of active users per AP. Here, we used inequality (35) and set $\alpha_m \times K_m = 100$. As Fig. 10 shows, the optimum value of K_m, (K_m^{opt}) is achieved by $K_m^{\text{opt}} = 33$. As a result, the proposed user assignment scheme can effectively improve the energy efficiency performance of cell-free Massive MIMO systems with limited backhaul capacity.

VIII. Conclusions

We have considered cell-free Massive MIMO when the quantized version of the weighted signals are available at the CPU. Bussgang decomposition has been used to model the quantization effects. A closed-form expression for spectral efficiency has been derived. We have then studied the problem of the energy efficiency maximization with per-user power constraints, backhaul capacity constraints and throughput requirements. We have developed an SCA to efficiently solve this non-convex problem. Next a low-complexity sub-optimal scheme is proposed. In addition, complexity and convergence of the proposed schemes have been investigated. Numerical results confirmed that the limited-backhaul cell-free Massive MIMO system with the proposed algorithm can reach almost twice the uplink total energy efficiency compared to the case of equal power allocation. In addition, a trade-off between the total number of APs and the number of antennas at the APs has been shown. Moreover, we investigated the optimal number of AP antennas along with the optimal number of quantization bits to maximize the uplink total energy efficiency of cell-free Massive MIMO. Finally, we have presented the energy efficiency performance as a function of relative loss in the max-min spectral efficiency and evaluated the energy efficiency improvement achieved by sacrificing some of the max-min spectral efficiency.

Appendix A: Proof of Theorem 1

The desired signal for the user k is given by

$$\mathrm{DS}_k = \sqrt{\rho}\mathbb{E}\left\{\sum_{m=1}^{M} u_{mk}\hat{\mathbf{g}}_{mk}^H \mathbf{g}_{mk}\sqrt{q_k}\right\} = N\sqrt{pq_k}\sum_{m=1}^{M} u_{mk}\gamma_{mk}. \tag{42}$$

Hence, $|\mathrm{DS}_k|^2 = \rho q_k \left(N\sum_{m=1}^{M} u_{mk}\gamma_{mk}\right)^2$. Moreover, the term $\mathbb{E}\{|\mathrm{BU}_k|^2\}$ can be obtained as

$$\mathbb{E}\left\{|\mathrm{BU}_k|^2\right\} = \rho\mathbb{E}\left\{\left|\sum_{m=1}^{M} u_{mk}\hat{\mathbf{g}}_{mk}^H \mathbf{g}_{mk}\sqrt{q_k} - \mathbb{E}\left\{\sum_{m=1}^{M} u_{mk}\hat{\mathbf{g}}_{mk}^H \mathbf{g}_{mk}\sqrt{q_k}\right\}\right|^2\right\} = \rho N\sum_{m=1}^{M} q_k u_{mk}^2 \gamma_{mk}\beta_{mk}, \tag{43}$$

where the last equality comes from the analysis in [3, Appendix A], and using $\gamma_{mk} = \sqrt{\tau_p p_p}\beta_{mk}c_{mk}$. The term $\mathbb{E}\{|\mathrm{IUI}_{kk'}|^2\}$ is obtained as

$$\begin{aligned}\mathbb{E}\{|\mathrm{IUI}_{kk'}|^2\} = &\underbrace{\rho\, q_{k'}\mathbb{E}\left\{\left|\sum_{m=1}^{M} c_{mk}u_{mk}\mathbf{g}_{mk'}^H \tilde{\mathbf{w}}_{mk}\right|^2\right\}}_{A} \\ &+\underbrace{\rho\tau_p p_p \mathbb{E}\left\{q_{k'}\left|\sum_{m=1}^{M} c_{mk}u_{mk}\Big(\sum_{i=1}^{K}\mathbf{g}_{mi}\boldsymbol{\phi}_k^H\boldsymbol{\phi}_i\Big)^H \mathbf{g}_{mk'}\right|^2\right\}}_{B},\end{aligned} \tag{44}$$

where the third equality in (44) is due to the fact that for two independent random variables X and Y and $\mathbb{E}\{X\}=0$, we have $\mathbb{E}\{|X+Y|^2\}=\mathbb{E}\{|X|^2\}+\mathbb{E}\{|Y|^2\}$ [3]. Since $\tilde{\mathbf{w}}_{mk}=\boldsymbol{\phi}_k^H\mathbf{W}_{\mathbf{p},\mathbf{m}}$ is independent of the term $g_{mk'}$ similar to [3, Appendix A], the term A in (44) immediately is given by $A=Nq_{k'}\sum_{m=1}^{M}c_{mk}^2u_{mk}^2\beta_{mk'}$. The term B in (44) can be obtained as

$$B=\underbrace{\tau_p p_p q_{k'}\mathbb{E}\left\{\left|\sum_{m=1}^{M}c_{mk}u_{mk}||\mathbf{g}_{mk'}||^2\boldsymbol{\phi}_k^H\boldsymbol{\phi}_{k'}\right|^2\right\}}_{C}+\underbrace{\tau_p p_p q_{k'}\mathbb{E}\left\{\left|\sum_{m=1}^{M}c_{mk}u_{mk}\Big(\sum_{i\neq k'}^{K}\mathbf{g}_{mi}\boldsymbol{\phi}_k^H\boldsymbol{\phi}_i\Big)^H\mathbf{g}_{mk'}\right|^2\right\}}_{D}. \quad (45)$$

The first term in (45) is given by

$$C=N\tau_p p_p q_{k'}\left|\boldsymbol{\phi}_k^H\boldsymbol{\phi}_{k'}\right|^2\sum_{m=1}^{M}c_{mk}^2u_{mk}^2\beta_{mk'}+N^2q_{k'}\left|\boldsymbol{\phi}_k^H\boldsymbol{\phi}_{k'}\right|^2\left(\sum_{m=1}^{M}u_{mk}\gamma_{mk}\frac{\beta_{mk'}}{\beta_{mk}}\right)^2, \quad (46)$$

where the last equality is derived based on the fact that $\gamma_{mk}=\sqrt{\tau_p p_p}\beta_{mk}c_{mk}$. The second term in (45) can be obtained as

$$D=N\sqrt{\tau p_p}q_{k'}\sum_{m=1}^{M}u_{mk}^2c_{mk}\beta_{mk'}\beta_{mk}-Nq_{k'}\sum_{m=1}^{M}u_{mk}^2c_{mk}^2\beta_{mk'}-N\tau p_p q_{k'}\sum_{m=1}^{M}u_{mk}^2c_{mk}^2\beta_{mk'}^2\left|\boldsymbol{\phi}_k^H\boldsymbol{\phi}_{k'}\right|^2. \quad (47)$$

Finally by substituting (46) and (47) into (45), and substituting (45) into (44), we obtain

$$\mathbb{E}\{|\mathrm{IUI}_{kk'}|^2\}=N\rho q_{k'}\left(\sum_{m=1}^{M}u_{mk}^2\beta_{mk'}\gamma_{mk}\right)+N^2\rho q_{k'}\left|\boldsymbol{\phi}_k^H\boldsymbol{\phi}_{k'}\right|^2\left(\sum_{m=1}^{M}u_{mk}\gamma_{mk}\frac{\beta_{mk'}}{\beta_{mk}}\right)^2. \quad (48)$$

The total noise for the user k is given by

$$\mathbb{E}\left\{|\mathrm{TN}_k|^2\right\}=\mathbb{E}\left\{\left|\sum_{m=1}^{M}u_{mk}\hat{\mathbf{g}}_{mk}^H\mathbf{n}_m\right|^2\right\}=N\sum_{m=1}^{M}u_{mk}^2\gamma_{mk}, \quad (49)$$

where the last equality is due to the fact that the terms $\hat{\mathbf{g}}_{mk}$ and $\mathbf{n}_m$ are uncorrelated. The power of the quantization distortion for user k is given by

$$\mathbb{E}\left\{|\mathrm{TQD}_k|^2\right\}=\mathbb{E}\left\{\left|\sum_{m=1}^{M}u_{mk}n_{d,mk}\right|^2\right\}. \quad (50)$$

In general, the inputs of the quantizers at different APs are correlated, and hence, the quantization distortions across APs are correlated. However, analysis and numerical results for typical cases based on [54]–[56] show that:

$$\mathbf{R}_{\mathbf{n}_{d,k}\mathbf{n}_{d,k}}\approx\underbrace{\left(\tilde{b}-\tilde{a}^2\right)}_{\sigma_{\tilde{e}}^2}\mathrm{diag}(\mathbf{R}_{\mathbf{z}_k\mathbf{z}_k}), \quad (51)$$

where $\mathbf{R}_{\mathbf{n}_{d,k}\mathbf{n}_{d,k}}=\mathbb{E}\left\{\mathbf{n}_{d,k}\mathbf{n}_{d,k}^H\right\}$ and $\mathbf{R}_{\mathbf{z}_k\mathbf{z}_k}=\mathbb{E}\left\{\mathbf{z}_k\mathbf{z}_k^H\right\}$ refer to the covariance matrix of the quantization distortion and the covariance matrix of the input of quantizer, respectively. This

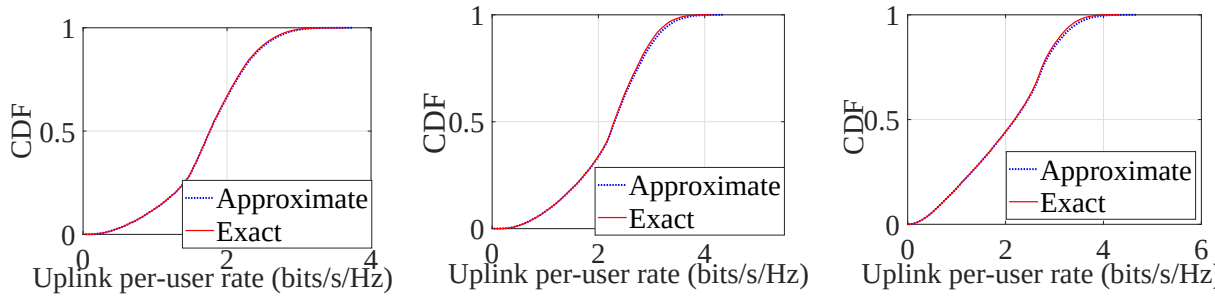

(a) $M = 60$, $N = 4$, $K = 20$, and $\tau_p = 20$. (b) $M = 80$, $N = 4$, $K = 30$, and $\tau_p = 30$. (c) $M = 60$, $N = 6$, $K = 40$, and $\tau_p = 30$.

Figure 11. Uplink per-user rate of cell-free Massive MIMO with. Here, the term "Exact" refers to the case where we use the exact result (50), whereas the term "Approximate" refers to the case we use the approximation (52). In all figures, we set $\alpha = 2$ quantization bits, and use equal power allocation.

implies that the quantization distortions across APs can be assumed to by uncorrelated. Therefore, we can obtain the following approximation

$$\mathbb{E}\left\{|\mathrm{TQD}_k|^2\right\} = \mathbb{E}\left\{\left|\sum_{m=1}^{M} u_{mk} n_{d,mk}\right|^2\right\} \approx \sum_{m=1}^{M} u_{mk}^2 \mathbb{E}\left\{|n_{d,mk}|^2\right\}. \tag{52}$$

Note that the numerical analysis in [23] show that for the case of small number of users, the correlation affects the spectral efficiency performance of the massive MIMO system. However, for cell-free Massive MIMO, under the conditions listed below, the quantization distortions are approximately uncorrelated: 1) There is no line-of-sight (LOS) component, 2) having large path loss differences at different APs to avoid large correlation, 3) having a large number of users, and 4) having small N. To validate the approximation (52), we next present the uplink per-user rate with different system parameters for two different scenarios; 1) the exact uplink per-user rate with $\mathbb{E}\left\{|\mathrm{TQD}_k|^2\right\} = \mathbb{E}\left\{\left|\sum_{m=1}^{M} u_{mk} n_{d,mk}\right|^2\right\}$, which is referred to as "Exact" in Fig. 11a-11c; and 2) the uplink per-user rate with $\mathbb{E}\left\{|\mathrm{TQD}_k|^2\right\} = \sum_{m=1}^{M} u_{mk}^2 \mathbb{E}\left\{|n_{d,mk}|^2\right\}$, where refers to the case when we ignore the correlation between the inputs of the quantizers, and this scenario is given as "Approximate" in Fig. 11a-11c. As Fig. 11a-11c shows, there is a negligible performance gap between the exact SINR and the approximate SINR. To calculate the power of the quantization distortion, given by (52), we use the following property of the quantization distortion power

$$\mathbb{E}\left\{|n_{d,mk}|^2\right\} = \sigma^2_{\hat{\mathbf{g}}_{mk}^H \mathbf{y}_m} \mathbb{E}\left\{|\tilde{n}_{d,mk}|^2\right\}. \tag{53}$$

where the term $\sigma^2_{\hat{\mathbf{g}}_{mk}^H \mathbf{y}_m}$ is

$$\sigma^2_{\hat{\mathbf{g}}_{mk}^H \mathbf{y}_m} = \sigma^2_{z_{mk}} = \mathbb{E}\left\{|z_{mk}|^2\right\} = N^2 \sum_{k'=1}^{K} \gamma^2_{mk'} \left|\boldsymbol{\phi}_{k'}^H \boldsymbol{\phi}_k\right|^2 \rho q_{k'} + N\gamma_{mk} \sum_{k'=1}^{K} \beta_{mk'} \rho q_{k'} + N\gamma_{mk}. \tag{54}$$

Therefore, we have

$$\mathbb{E}\left\{|\mathrm{TQD}_k|^2\right\}=\underbrace{\left(\tilde{b}-\tilde{a}^2\right)}_{\sigma_{\tilde{e}}^2}\sum_{m=1}^{M}u_{mk}^2\left(N^2\sum_{k'=1}^{K}\gamma_{mk'}^2\left|\boldsymbol{\phi}_{k'}^H\boldsymbol{\phi}_k\right|^2\rho q_{k'}+N\gamma_{mk}\sum_{k'=1}^{K}\beta_{mk'}\rho q_{k'}+N\gamma_{mk}\right). \quad (55)$$

By substituting (42), (43), (48), (49) and (55) into (11), the corresponding SINR of the kth user is obtained by (12), which completes the proof of Theorem 1. ■

APPENDIX B: DETAILS OF FINDING ν^* IN REMARK 2

Assuming a total transmit power of $\sum_{k=1}^{K}q_k$, the power minimization problem can be defined as follows:

$$P_{13}: \quad \min_{q_k} \quad \sum_{k=1}^{K}q_k \quad (56a)$$

$$\text{s.t.} \quad S_k\left(q_k,\mathbf{u}_k,\alpha\right)\geq S_k^{(\mathrm{r})}, \quad \forall k,\ 0\leq q_k\leq p_{\max}^{(k)},\forall k. \quad (56b)$$

Problem P_{13} is a GP and can be efficiently solved. After solving Problem P_{13} and finding the optimal solution $q_k^+,\forall k$, the slack variable ν^* is obtained as follows:

$$\nu^*=\frac{\sum_{k=1}^{K}p_{\max}^{(k)}}{\sum_{k=1}^{K}q_k^+}, \quad (57)$$

which completes the definition for Remark 2. ■

APPENDIX C: PROOF OF PROPOSITION 1

The standard form of GP is defined as follows [47], [57]:

$$P_{14}: \quad \min \quad f_0(\mathbf{x}), \quad (58a)$$

$$\text{s.t.} \quad f_i(\mathbf{x})\leq 1, \quad i=1,\cdots,m,\ g_i(\mathbf{x})=1, \quad i=1,\cdots,p, \quad (58b)$$

where f_0 and f_i are posynomial and g_i are monomial functions. Moreover, $\mathbf{x}=\{x_1,\cdots,x_n\}$ represents the optimization variables. The SINR constraint in (58) is not a posynomial function in its initial form, however it can be rewritten into the following posynomial function:

$$\frac{\mathbf{u}_k^H\left(N^2\sum_{k'\neq k}^{K}q_{k'}|\boldsymbol{\phi}_k^H\boldsymbol{\phi}_{k'}|^2\boldsymbol{\Delta}_{kk'}\boldsymbol{\Delta}_{kk'}^H+N^2\sum_{k'=1}^{K}q_{k'}|\boldsymbol{\phi}_k^H\boldsymbol{\phi}_{k'}|^2\boldsymbol{\Lambda}_{k'}+N\sum_{k'=1}^{K}q_{k'}\mathbf{D}_{kk'}+\frac{N}{\rho}\mathbf{R}_k\right)\mathbf{u}_k}{\mathbf{u}_k^H\left(N^2q_k\boldsymbol{\Gamma}_k\boldsymbol{\Gamma}_k^H\right)\mathbf{u}_k}\leq\frac{1}{t},\ \forall k. \quad (59)$$

By applying a simple transformation, (59) is equivalent to the following inequality:

$$q_k^{-1}\left(\sum_{k'\neq k}^{K}a_{kk'}q_{k'}+\sum_{k'=1}^{K}b_{kk'}q_{k'}+\sum_{k'=1}^{K}e_{kk'}q_{k'}+c_k\right)\leq\frac{1}{t}, \quad (60)$$

where $a_{kk'}=\frac{\mathbf{u}_k^H\left(\left|\boldsymbol{\phi}_k^H\boldsymbol{\phi}_{k'}\right|^2\boldsymbol{\Delta}_{kk'}\boldsymbol{\Delta}_{kk'}^H\right)\mathbf{u}_k}{\mathbf{u}_k^H\left(\boldsymbol{\Gamma}_k\boldsymbol{\Gamma}_k^H\right)\mathbf{u}_k}$, $b_{kk'}=\frac{\mathbf{u}_k^H\mathbf{D}_{kk'}\mathbf{u}_k}{\mathbf{u}_k^H\left(N\boldsymbol{\Gamma}_k\boldsymbol{\Gamma}_k^H\right)\mathbf{u}_k}$, $e_{kk'}=\frac{\mathbf{u}_k^H\left(\left|\boldsymbol{\phi}_k^H\boldsymbol{\phi}_{k'}\right|^2\boldsymbol{\Lambda}_{k'}\right)\mathbf{u}_k}{\mathbf{u}_k^H\left(\boldsymbol{\Gamma}_k\boldsymbol{\Gamma}_k^H\right)\mathbf{u}_k}$ and $c_k=\frac{\mathbf{u}_k^H\mathbf{R}_k\mathbf{u}_k}{\mathbf{u}_k^H\left(\rho N\boldsymbol{\Gamma}_k\boldsymbol{\Gamma}_k^H\right)\mathbf{u}_k}$. The transformation in (60) shows that the left-hand side of (59) is a posynomial

function. Moreover, the spectral efficiency constraint in (29b) is not a posynomial function in its original form, however, through some mathematical manipulation, it can be written as:

$$\frac{\mathbf{u}_k^H \left(N^2 \sum_{k' \neq k}^{K} q_{k'} |\boldsymbol{\phi}_k^H \boldsymbol{\phi}_{k'}|^2 \boldsymbol{\Delta}_{kk'} \boldsymbol{\Delta}_{kk'}^H + N^2 \sum_{k'=1}^{K} q_{k'} |\boldsymbol{\phi}_k^H \boldsymbol{\phi}_{k'}|^2 \boldsymbol{\Lambda}_{k'} + N \sum_{k'=1}^{K} q_{k'} \mathbf{D}_{kk'} + \frac{N}{\rho} \mathbf{R}_k \right) \mathbf{u}_k}{\mathbf{u}_k^H \left(N^2 q_k \boldsymbol{\Gamma}_k \boldsymbol{\Gamma}_k^H\right) \mathbf{u}_k} \leq \frac{1}{\hat{S}_k^{(\mathrm{r})}}, \ \forall k, \quad (61)$$

where $\hat{S}_k^{(\mathrm{r})} = 2^{\frac{\tau_c S_k^{(\mathrm{r})}}{\tau_c - \tau_p}} - 1$. By applying a simple transformation, (61) is equivalent to the following inequality:

$$q_k^{-1} \left(\sum_{k' \neq k}^{K} a_{kk'} q_{k'} + \sum_{k'=1}^{K} b_{kk'} q_{k'} + \sum_{k'=1}^{K} e_{kk'} q_{k'} + c_k \right) \leq \frac{1}{\hat{S}_k^{(\mathrm{r})}}. \quad (62)$$

Therefore, the power allocation problem P_6 is a standard GP (convex problem), where the objective function and constraints are monomial and posynomial, respectively, which completes the proof of Proposition 1. ■

APPENDIX D: PROOF OF PROPOSITION 3

Let us consider the following GP problem:

$$P^{\mathrm{GP}} : \min f_0(\mathbf{x}) = \sum_{i \in \mathcal{I}_0} c_{i0} \exp\{a_i^T \mathbf{x}\} \quad \text{s.t. } f_j(\mathbf{x}) = \sum_{i \in \mathcal{I}_j} c_{ij} \exp\{a_i^T \mathbf{x}\} \leq d_j, j = 1, \cdots, n_3, \quad (63)$$

where $\mathbf{x} = \{x_1, \cdots, x_{n_1}\}$ represents the optimization variables, $\mathcal{I}_j$ are subset of the index set $\mathcal{I} = 1, \cdots, n_2$, and all coefficients c_{ij} are positive, $j = 1, \cdots, n_3$ [58, Chapter 10]. Based on the analysis in [58, Chapter 10], the complexity of solving the GP problem given in (63) is given by $\mathcal{C} = \mathcal{O}\left((n_2 + n_3)^{\frac{1}{2}} (n_3 n_2^2 + n_2^3 + n_1^3)\right)$. Therefore, exploiting P_{11} defined in (32) and the transformation in (59)-(62), we have $n_1 = K$, $n_2 = 2K - 1$ and $n_3 = 2K$. Note that $n_2 = 2K - 1$ is obtained using the transformation in (62) for the constraint in (32b), and also the transformation in (60) for constraint (32d). Hence, Problem P_{11}, can be solved with a complexity equivalent to $n_{\text{iter}} \times \mathcal{O}\left((2K - 1 + 2K)^{\frac{1}{2}} \left((2K)(2K-1)^2 + (2K-1)^3 + (2K)^3\right)\right)$, where n_{iter} refers to the number of iterations to solve P_{11} which depends on δ in (32f). Moreover, it can be shown that Problem P_{12} can be solved with a complexity of $\mathcal{O}\Big((2K-1+2K)^{\frac{1}{2}} \left((2K)(2K-1)^2 + (2K-1)^3 + (2K)^3\right)\Big)$. After some manipulations, we end up with the values given in Table II, which completes the proof of Proposition 3. ■

REFERENCES

[1] M. Bashar, K. Cumanan, A. G. Burr, , H. Q. Ngo, and E. G. Larsson, "On the energy efficiency of limited-backhaul cell-free Massive MIMO," in *Proc. IEEE ICC*, May 2019, pp. 1–7.

[2] Y. Xu, G. Yue, and S. Mao, "User grouping for Massive MIMO in FDD systems: New design methods and analysis," *IEEE Trans. Wireless Commun.*, vol. 14, no. 12, pp. 6827–6842, Jul. 2015.

[3] H. Q. Ngo, A. Ashikhmin, H. Yang, E. G. Larsson, and T. L. Marzetta, "Cell-free Massive MIMO versus small cells," *IEEE Trans. Wireless Commun.*, vol. 16, no. 3, pp. 1834–1850, Mar. 2017.

[4] E. Nayebi, A. Ashikhmin, T. L. Marzetta, H. Yang, and B. D. Rao, "Precoding and power optimization in cell-free Massive MIMO systems," *IEEE Trans. Wireless Commun.*, vol. 16, no. 7, pp. 4445–4459, Jul. 2017.

[5] M. Bashar, K. Cumanan, A. G. Burr, H. Q. Ngo, and H. V. Poor, "Mixed quality of service in cell-free Massive MIMO," *IEEE Commun. Lett.*, vol. 22, no. 7, pp. 706–709, Jul. 2018.

[6] S. Buzzi and C. DAndrea, "Cell-free Massive MIMO: user-centric approach," *IEEE Wireless Commun. Lett.*, vol. 6, no. 6, pp. 1–4, Aug. 2017.

[7] G. Interdonato, E. Bjornson, H. Q. Ngo, P. Frenger, and E. G. Larsson, "Ubiquitous cell-free Massive MIMO communications," *[online]. Available:https://arxiv.org/pdf/1804.03421.pdf*, pp. 1–19, Submitted to IEEE Commun. Mag.

[8] J. Zhang, Y. Wei, E. Björnson, Y. Han, and S. Jin, "Performance analysis and power control of cell-free Massive MIMO systems with hardware impairments," *IEEE Access*, vol. 6, pp. 55 302–55 314, Sep. 2018.

[9] M. K. Karakayali, G. J. Foschini, and R. A. Valenzuela, "Network coordination for spectrally efficient communications in cellular systems," *IEEE Trans. Wireless Commun.*, vol. 13, no. 4, pp. 56–61, Aug. 2006.

[10] D. Gesbert, S. Hanly, H. Huang, S. S. Shitz, O. Simeone, and W. Yu, "Multi-cell MIMO cooperative networks: A new look at interference," *IEEE J. Sel. Areas Commun.*, vol. 28, no. 9, pp. 1380–1408, Dec. 2010.

[11] S. Shamai and B. M. Zaidel, "Enhancing the cellular downlink capacity via co-processing at the transmitting end," in *Proc. IEEE VTC*, May 2001, pp. 1745–1749.

[12] E. Bjornson, R. Zakhour, D. Gesbert, and B. Ottersten, "Cooperative multicell precoding: Rate region characterization and distributed strategies with instantaneous and statistical CSI," *IEEE Trans. Signal Process.*, vol. 58, no. 8, pp. 4298–4310, Aug. 2010.

[13] O. Simeone, O. Somekh, H. V. Poor, and S. Shamai, "Downlink multicell processing with limited-backhaul capacity," *EURASIP J. Adv. in Signal Process.*, no. 1, pp. 814–840, Jun. 2009.

[14] P. Marsch and G. Fettweis, "On multicell cooperative transmission in backhaul-constrained cellular systems," *Ann. Telecommun.*, vol. 63, no. 5, pp. 253–269, Jan. 2008.

[15] Z. Chen and E. Björnson, "Channel hardening and favorable propagation in cell-free Massive MIMO with stochastic geometry," *IEEE Trans. Commun.*, vol. 66, no. 11, pp. 5205–5219, Nov. 2018.

[16] Z. Gao, L. Dai, D. Mi, Z. Wang, M. A. Imran, and M. Z. Shakir, "MmWave Massive-MIMO-based wireless backhaul for the 5G ultra-dense network," *IEEE Trans. Wireless Commun.*, vol. 22, no. 5, pp. 13–21, Oct. 2015.

[17] A. G. Burr, M. Bashar, and D. Maryopi, "Cooperative access networks: Optimum fronthaul quantization in distributed Massive MIMO and cloud RAN," in *Proc. IEEE VTC*, Jun. 2018, pp. 1–7.

[18] A. Burr, M. Bashar, and D. Maryopi, "Ultra-dense radio access networks for smart cities: Cloud-RAN, Fog-RAN and cell-free Massive MIMO," in *Proc. IEEE PIMRC*, Sep. 2018.

[19] *Common Public Radio Interface (CPRI)*. Interface Specification V6.0, Aug 2013.

[20] T. Rep, *C-RAN: the road towards green RAN*. China Mobile Research Institute, Oct 2011.

[21] J. Zhang, L. Dai, Z. He, S. Jin, and X. Li, "Performance analysis of mixed-ADC Massive MIMO systems over Rician fading channels," *IEEE J. Sel. Areas Commun.*, vol. 35, no. 6, pp. 1327–1338, Jun. 2017.

[22] J. Zhang, L. Dai, X. Li, Y. Liu, and L. Hanzo, "On low-resolution ADCs in practical 5G millimeter-wave Massive MIMO systems," *IEEE Commun. Mag.*, vol. 56, no. 7, pp. 205–211, Jul. 2018.

[23] E. Björnson, L. Sanguinetti, and J. Hoydis, "Hardware distortion correlation has negligible impact on UL Massive MIMO spectral efficiency," *IEEE Trans. Commun.*, vol. 67, no. 2, pp. 1085–1098, Feb. 2019.

[24] P. Zillmann, "Relationship between two distortion measures for memoryless nonlinear systems," *IEEE Signal Process. Lett.*, vol. 17, no. 11, pp. 917–920, Feb. 2010.

[25] A. J. Fehske, P. Marsch, and G. P. Fettweis, "Bit per joule efficiency of cooperating base stations in cellular networks," in *Proc. IEEE Globecom Workshops*, Dec. 2010, pp. 1406–1411.

[26] H. Q. Ngo, H. Tataria, M. Matthaiou, S. Jin, and E. G. Larsson, "On the performance of cell–free Massive MIMO in Ricean fading," in *Proc. IEEE Asilomar*, Nov. 2018, pp. 1–6.

[27] J. Zhang, L. Dai, S. Sun, and Z. Wang, "On the spectral efficiency of Massive MIMO systems with low-resolution ADCs," *IEEE Commun. Lett.*, vol. 20, no. 5, pp. 842–845, May 2016.

[28] T. S. Rappaport, *Wireless Communications: Principles and Practice*. Englewood Cliffs, NJ, USA: Prentice-Hall, 2002.

[29] A. Ashikhmin, T. L. Marzetta, and L. Li, "Interference reduction in multi-cell Massive MIMO systems I: Large-scale fading precoding and decoding," *Available: https://arxiv.org/abs/1411.4182*, Submitted to IEEE Trans. Inf. Theory.

[30] M. Bashar, K. Cumanan, A. G. Burr, H. Q. Ngo, and M. Debbah, "Max-min SINR of cell-free Massive MIMO uplink with optimal uniform quantization," *IEEE Trans. Commun.*, submitted.

[31] M. Bashar, H. Q. Ngo, A. Burr, D. Maryopi, K. Cumanan, and E. G. Larsson, "On the performance of backhaul constrained cell-free Massive MIMO with linear receivers," in *Proc. IEEE Asilomar*, Nov. 2018, pp. 1–7.

[32] D. Maryopi, M. Bashar, and A. Burr, "On the uplink throughput of zero-forcing in cell-free Massive MIMO with coarse quantization," *IEEE Trans. Veh. Technol.*, pp. 1–5, Jun. 2019.

[33] J. J. Bussgang, *Crosscorrelation functions of amplitude-distorted gaussian signals*. MIT research LabElectron Cambridge, MA, USA, 1952.

[34] A. V. Oppenheim, R. W. Schafer, and J. R. Buck, *Discrete-time signal processing*. Prentice-hall Englewood Cliffs, 1989.

[35] J. Max, "The worst additive noise under a covariance constraint," *IEEE Trans. Inf. Theory*, vol. 6, no. 1, pp. 7–12, Nov. 1960.

[36] A. Kakkavas, J. Munir, A. Mezghani, H. Brunner, and J. A. Nossek, "Weighted sum rate maximization for multiuser MISO systems with low resolution digital to analog converters," in *Proc. IEEE WSA*, Mar. 2016.

[37] J. G. Proakis, *Digital Communications*. McGraw-Hill, 1995.

[38] E. Björnson, L. Sanguinetti, J. Hoydis, and M. Debbah, "Optimal design of energy-efficient multi-user MIMO systems: Is Massive MIMO the answer?" *IEEE Trans. Wireless Commun.*, vol. 14, no. 6, pp. 3059–3075, Jun. 2015.

[39] O. Onireti, F. Heliot, and M. A. Imran, "On the energy efficiency-spectral efficiency trade-off of distributed MIMO systems," *IEEE Trans. Commun.*, vol. 61, no. 9, pp. 3741–3753, Sep. 2013.

[40] ——, "On the energy efficiency-spectral efficiency trade-off in the uplink of CoMP system," *IEEE Trans. Commun.*, vol. 11, no. 2, pp. 556–561, Feb. 2012.

[41] L. Falconetti and E. Yassin, "Towards energy efficiency with uplink cooperation in heterogeneous networks," in *Proc. IEEE WCNC*, Apr. 2014, pp. 1649–1654.

[42] S. He, Y. Huang, L. Yang, B. Ottersten, and W. Hong, "Energy efficient coordinated beamforming for multicell system: duality-based algorithm design and Massive MIMO transition," *IEEE Trans. Commun.*, vol. 63, no. 12, pp. 4920–4935, Dec. 2013.

[43] H. Dahrouj and W. Yu, "Coordinated beamforming for the multicell multi-antenna wireless system," *IEEE Trans. Wireless Commun.*, vol. 9, no. 5, pp. 1748–1759, Jan. 2010.

[44] G. Golub and C. V. Loan, *Matrix Computations*, 2nd ed. Baltimore, MD: The Johns Hopkins Univ. Press, 1996.

[45] M. Bashar, K. Cumanan, A. G. Burr, , M. Debbah, and H. Q. Ngo, "Enhanced max-min SINR for uplink cell-free Massive MIMO systems," in *Proc. IEEE ICC*, May 2018, pp. 1–6.

[46] M. Bashar, K. Cumanan, A. G. Burr, M. Debbah, and H. Q. Ngo, "On the uplink max-min SINR of cell-free Massive MIMO systems," *IEEE Trans. Wireless Commun.*, vol. 18, no. 4, pp. 2021–2036, Apr. 2019.

[47] S. P. Boyd, S. J. Kim, A. Hassibi, and L. Vandenbarghe, "A tutorial on geometric programming," *Optim. Eng.*, vol. 8, no. 1, pp. 67–128, Apr. 2007.

[48] P. C. Weeraddana, M. Codreanu, M. Latva-aho, and A. Ephremides, "Resource allocation for cross-layer utility maximization in wireless networks," *IEEE Trans. Veh. Technol.*, vol. 60, no. 6, pp. 2790–2809, Jul. 2011.

[49] E. Björnson and E. Jorswieck, *Optimal Resource Allocation in Coordinated Multi-Cell Systems*. Foundations and Trends in Communications and Information Theory, 2012.

[50] H. Q. Ngo, L. Tran, T. Q. Duong, M. Matthaiou, and E. G. Larsson, "On the total energy efficiency of cell-free Massive MIMO," *IEEE Trans. Green Commun. and Net.*, vol. 2, no. 1, pp. 25–39, Mar. 2017.

[51] K. Cumanan, L. Musavian, S. Lambotharan, and A. B. Gershman, "SINR balancing technique for downlink beamforming in cognitive radio networks," *IEEE Signal Process. Lett.*, vol. 17, no. 2, pp. 133–136, Feb. 2010.

[52] P. Arbenz, *Lecture Notes on Solving Large Scale Eigenvalue Problems*, [online]. available:https:https://people.inf.ethz.ch/arbenz/ewp/lnotes/lsevp.pdf ed. Computer Science Department, ETH Zurich, 2016.

[53] M. Bashar, K. Cumanan, A. G. Burr, H. Q. Ngo, and M. Debbah, "Cell-free Massive MIMO with limited backhaul," in *Proc. IEEE ICC*, May 2018, pp. 1–7.

[54] R. Price, "A useful theorem for nonlinear devices having gaussian inputs," *IEEE Trans. Inf. Theory*, vol. 4, no. 2, pp. 69–72, Jun. 1958.

[55] Y. Li, C. Tao, G. Seco-Granados, A. Mezghani, A. L. Swindlehurst, and L. Liu, "Channel estimation and performance analysis of one-bit Massive MIMO systems," *IEEE Trans. Signal Process.*, vol. 65, no. 15, pp. 4075–4089, Aug. 2017.

[56] A. Mezghani and J. A. Nossek, "Capacity lower bound of MIMO channels with output quantization and correlated noise," in *Proc. IEEE ISIT*, Aug. 2012, pp. 1–5.

[57] S. Boyd and L. Vandenberghe, *Convex Optimization*. Cambridge, UK: Cambridge University Press, 2004.

[58] Y. Nesterov and A. Nemirovsky, *Interior-point polynomial methods in convex programming*. Studies in Applied Mathematics, SIAM, Philadelphia, 1994.